University of Nigeria

Research Publications

Author	AZUBUIKE, Josephine Onyemaechi
	PG/M.Sc/89/79541
Title	Design Construction and Characterization of Improved Local Pyranometer for the Measurement of Solar Intensity at Nsukka
Faculty	Physical Sciences
Department	Physics and Astronomy
Date	June, 1991
Signature	

DESIGN, CONSTRUCTION AND CHARACTERIZATION OF IMPROVED LOCAL PYRANOMETER FOR THE MEASUREMENT OF SOLAR INTENSITY AT NSUKKA

A PROJECT REPORT PRESENTED TO

THE DEPARTMENT OF PHYSICS AND ASTRONOMY,

UNIVERSITY OF NIGERIA, NSUKKA,

IN PARTIAL FULFILMENT OF THE REQUIREMENTS FOR THE AWARD OF THE DEGREE OF MASTER OF SCIENCE

BY

AZUBUIKE, JOSEPHINE ONYEMAECHI
(PG/M.Sc./89/7954)

SUPERVISORS:

1. DR C.E. OKEKE
   (ASSOCIATE PROF. OF PHYSICS)
   DEPT. OF PHYSICS AND ASTRONOMY
   U. N. N.

2. PROF. A.O.E. ANIMALU
   (PROF. OF PHYSICS)
   DEPT. OF PHYSICS AND ASTRONOMY
   U. N. N.

JUNE, 1991.

C E R T I F I C A T I O N

Miss Azubuike, J.O., a postgraduate student in the Department of Physics and Astronomy and with Reg. No. PG./M.Sc/89/7954 has satisfactorily completed the requirements for course and research work for the degree of Master of Science (M.Sc) in Physics and Astronomy (Solar Energy Physics). The work embodied in this project report is original and has not been submitted in part or full for any other diploma or degree of this or any other University.

DR. P. N. OKEKE
HEAD OF DEPARTMENT

DR. C. E. OKEKE
ASSOCIATE PROF. OF PHYSICS
(SUPERVISOR)

PROF. A.O.E. ANIMALU
PROF. OF PHYSICS
(SUPERVISOR)

C O N T E N T S

C O N T E N T S (Contd.)

ACKNOWLEDGEMENT

I wish to express my profound gratitude and appreciation for the fatherly assistance and help rendered to me by my project Supervisor, Dr. C.E. Okeke throughout the period of this research project work. Inspite of the load of work before him, he always found time at any point to attend to my problems.

I extend my thanks to Prof. A.O.E. Animalu who was also my project supervisor for his words of advice. He was a great source of inspiration and encouragement.

My sincere thanks also go to Dr. P.N. Okeke, the Head of Department of Physics and Astronomy. He was a tower of strength in my hours of doubt and uncertainty.

My thanks also go to Mr. P.I. Okolo of the Department of Physics and Astronomy, Mr. E.N. Ekezie of the Department of Chemistry, and Mr. A.U. Ekpo of Mechanical Engineering, all of University of Nigeria, Nsukka. These Chief Technologists in their various Departments helped immensely in various ways during the construction of the Pyranometer.

I also wish to thank Messrs Nwokoroku and Ozioko both of the Department of Physics and Astronomy for their technical assistance.

DEDICATION

This project is dedicated to my parents, MR. LAZARUS AZUBUIKE AND MRS ELIZABETH AZUBUIKE for their tremendous encouragement and unflinching moral and financial support. I owe them a world of gratitude.

ABSTRACT

Although Nigerians have hitherto viewed cheap and plentiful energy sources such as coal, oil and gas as their birth right, the supply is no longer cheap or accessible. There is an energy crisis due to political instability coupled with the drop in foreign exchange due to drop in oil export. The use of solar energy now becomes a viable option. To harness and utilize this abundant solar energy efficiently, it is necessary to know just how much of this energy is actually available at any given location and the factors that influence its intensity (including seasonal variations).

With this problem in mind, an improved thermopile pyranometer has been constructed using locally available materials and was used to measure the total (direct and diffuse) daily insolation at Nsukka (Latitude 6.8°N; Longitude 7.35°E) in May, 1991. The readings obtained clearly show that the constructed pyranometer is very sensitive and responds quickly to any fluctuations in solar radiation intensity.

Chapter one of this project work deals with the fundamental concept of the sun which is the source of solar energy. The factors that influence this solar energy distributions on Earth are also discussed.

In chapter two, some solar radiation Measuring Instruments and their characteristics are discussed. Chapter three gives full information on how the local pyranometer was successfully constructed, assembled and then checked.

Results from measurements in chapter four indicate that the daily insolation at the University of Nigeria, Nsukka in the month of May, 1991 had a highest mean instantaneous value of 491 WM^{-2} and a lowest value of 29 WM^{-2}. These results showed marked improvement on earlier pyranometers constructed by Eze and Asogwo[30]. The pyranometer was calibrated using standand Eppley pyranometer. Results of the calibration reveal that it has a calbration constant of $0.87mmV/WM^{-2} \pm 1.2\%$.

CHAPTER ONE

1.1 INTRODUCTION

In order to utilize solar energy successfully and efficiently, it is necessary to know how much of it is actually available at any given location and the factors that influence its intensity. Data on solar radiation is of great interest in characterising an area with respect to its agricultural potential, engineering design and analysis of solar processes, and in gaining some knowledge of the local climate.

To carry out such investigation, it is essential that a simple but sensitive equipment should be constructed preferably locally. The sophistication of some imported equipment makes their repair and maintenance problematic and a hinderance to smooth research work. Moreover, such equipment may have been designed to suit particular environmental conditions of the home country. Local manufacture of such equipment would eliminate most of the problems. This project is an attempt in this direction.

The design and assessment of the performance of any solar energy system requires a knowledge of solar radiation gained over a long period of time. However, most solar radiation stations generally record only total short wave radiation data on horizontal surfaces. Therefore, methods have to be devised to estimate the beam and diffuse components of total radiation on a horizontal surface.

Solar radiation is detected by interception and subsequent analysis of the effects of the interceptions on a receiver. Three possible ways in which the solar radiation can be sensed include:

i) By absorption and conversion to sensible heat.

ii) By the effect of a chemical process.

iii) By photon capture and conversion to electrical power.

From measurements made, empirical formulae have been developed over the years to estimate the solar radiation available using various parameters. Such methods include the correlation of insolation with meteorological parameters such as sun shine hours, air temperature and relative humidity.

1.2 THE NEED FOR HARNESSING SOLAR ENERGY

For generations, fossil fuels such as coal, oil and gas have been the only sources of energy supply. These fossil fuels have often been abundantly available to heat our homes, power our automobiles and fuel our industries. But, over a period of time, the supply of these fossils fuels began to dwindle and man began to look to the atom for salvation. It was also realised that those sources of energy supply cause a lot of environmental pollution resulting in the atmosphere being choked with smog, our rivers and shores streaked with oil. In the case of nuclear power plants, there is also concern over the possibility of radioactivity being released into the atmosphere in the event of an accident and, over the long term, problems of disposal of radioactive wastes from these plants. Thus, there is a need to deal with both energy shortages and environmental pollution in our homes and surroundings.

Americans were the first to discover the use of solar energy as one step toward reversing this trend. They found that a lot of energy can be trapped from the sun to heat and cool our homes thereby reducing the growing dependence on traditional energy sources that pollute the environment and create ecological problems.

Today, Scientists have recognised Solar Energy as a vital subject for study - a future possibility to reduce our economic problems. Solar heating and cooling are feasible today and not at some nebulous future dates.

It is clearly necessary that we must become more attune to our environments particularly those in the tropical parts of the globe if we are to make the best use of solar energy. As we embark upon this new era of solar architecture we should not forget the lessons of history. Although many of the old ways of using the energy from the sun require personal attention, they are reliable and cause little harm to the ecosphere. They have withstood the test of time through their simplicity and application to real human needs. Only when we have made every effort to use the sun's abundant energy in simple ways should we introduce new technologies - and then only sparingly, patiently and carefully.

1.3 FUNDAMENTAL CONCEPTS OF SOLAR RADIATION

1.3.1 ORIGIN OF SOLAR RADIATION

The sun is the source of solar energy. Nearly all known elements are present in the sun, however the main constituents are hydrogen and helium. These elements constitute about 80 per cent and 19 per cent respectively. The sun has a mass of 1991 ($\pm$0.002) X 10^{10}Kg and a radius of 6.960 ($\pm$0.001) X 10^{8}M. It is at a mean distance of 150 million kilometers from the earth.

The temperature of the core of the sun is estimated to about 2 X 10^{7}k while the outer most layer from which equivalent black - body termperature of 5760^{o}k.

The electromagnetic energy radiated by the sun is derived from nuclear fusion reactions in the sun. There are two sets of nuclear reactions that occur in the sun. These are the Proton - Proton chain and the Carbon - Nitrogen cycle. The reactions involved in the proton - proton chain are

$$ {}^{1}H + {}^{1}H \text{ —— } {}^{2}H + B + Y + 0.42 \text{ MeV.} $$

$$ {}^{1}H + {}^{2}H \text{ —— } {}^{3}He + Y + 5.5 \text{ Mev} $$

$$ {}^{3}He + {}^{3}He \text{ —— } {}^{4}He + \tfrac{1}{2}H + 12.8 \text{ Mev} $$

In the Carbon - Nitrogen cycle, the reactions are

$$ {}^{12}C + {}^{1}H \text{ —— } {}^{13}N + Y + 2 \text{ Mev} $$

$$ {}^{13}N \text{ —— } {}^{13}C + B + 0.5 \text{ Mev} $$

$$ {}^{13}C + {}^{1}H \text{ —— } 14N + Y + 8.2 \text{ MeV} $$

$$ {}^{14}N + {}^{1}H \text{ —— } {}^{15}O + Y + 7.5 \text{ MeV} $$

$$ {}^{15}O \text{ —— } {}^{15}N + B + Y + 0.7 \text{ MeV} $$

$$ {}^{15}N + {}^{1}H \text{ —— } {}^{12}C + {}^{4}He + 5.2 \text{ MeV} $$

The energy emitted by the sun results from the net mass change which accompanies the above reactions. The amount of energy resulting from a net mass change of ΔM is given by the Einstein relation,

$$ E = \Delta MC^2. $$

where

C is the velocity of light in a vacuum. It is estimated that the sun radiates energy into space at a rate of

approximately 4×10^{26} J S^{-1}. The earth intercepts only a small fraction of this energy, ranging from the ultra violet (uv) to the infra-red (IR) and radio spectral regions.
Of the total energy radiated by the sun only about 1.7×10^{13} J is intercepted by the earth every second.

1.3.2 EXTRA TERRESTRIAL SOLAR RADIATION

The solar radiation beyond the earth's atmosphere is called extra terrestrial solar radiation. The extra terrestrial solar radiation consists of beam (or direct) radiation only. Beam radiation is the solar radiation flux incident on a surface without significant change in direction or scattering.

In the Earth's atmosphere, the solar radiation interacts with the constituents of the atmosphere. This interaction results in a substantial modification of the in-coming extra terrestrial solar radiation both in intensity and in spectral distribution. The solar radiation is now referred to as terrestrial solar radiation.

Owing to the elliptical nature of the earth's orbit around the sun, the outskirts of the earth's atmosphere are not constant. The instantaneous extra terrestrial beam radiation differs from the solar constant by an orbital eccentricity factor, e, given by

$$e = 1 + 0.035 \cos \left[2 \pi (N-4)/365 \right] \quad ---(5)$$

where N is the day number from January 1. The extra terrestrial intensity on day N is the solar constant modulated by the orbital eccentricity factor i.e

$$Eo = E_{sc}\left[1 + 0.35Cos(2\Pi(N-4)/365)\right] \text{---}(6).$$

The total extra terrestrial solar radiation received by a horizontal surface over a time interval t is generally given by

$$E_t = \int_t^{t+\Delta t} E_o\ (N)\ Cosi\ (t)\ dt \text{--------}(7)$$

where i is the solar incidence angle given by

$$Cosi = SinL\ Sind + CosL\ Cosd\ CosLs + Sinx$$

(for a horizontal surface)

where L is the Latitude of the site, d is the solar declination, Ls is the hour angle and X is the solar altitude. The solar declination is defined as the angle at noon on the equator between the zenith and a line collinear with the sun's rays and is given by

$$d = 23.45\ Sin\left[360\ (N + 284)/365\right] \text{----}(9)$$

where N is the day of the year. The hour angle is obtained by multiplying the number of hours from the local solar noon by 15^o, i.e

$hs = 15^o$ x No. of hours from local solar noon.

At a given time, the instantaneous extra terrestrial beam insolation on a horizontal surface is

$$E_{oh} = E_{sc} \times \left[1 + 0.035\ Cos(2\Pi(N-4)/365)\right] \times$$
$$(SinLs\ Sind + CosL\ Cosd - Coshs)\text{---}(10)$$

The daily total extra terrestrial solar radiation is

$$E_{t,d} = \left(\frac{24}{\Pi}\right) E_{so}\left[1 + 0.034 \cos\left(\frac{2\Pi N}{365}\right)\right] (h_{sr} \sin L . \sin d + \cos L . \cos d . \sin h_{sr}) \text{ -------------- } (11)$$

where h_{sr} is the sun - rise hour angle.

1.3.4 THE SOLAR CONSTANT

The radiant power per unit area perpendicular to the direction of the sun outside the earth's atmosphere, but at the mean earth - sun distance is essentially constant. This radiation intensity is referred to as the solar constant or alternatively, air mass zero (AMO) radiation. The accepted value of the solar constant is 1353 w/m^2 ($\pm$ 1.6%). However, more recent measurements suggest that the value of the solar constant lies between 1368 and 1377 W/M^2. These values have been determined by taking a weighted average of measurements made by equipment mounted on ballons, high - altitude aircraft, and space crafts. As indicated by the two uppermost curves in figure 1.0, the spectral distribution of AMO radiation differs from that of an ideal black body. This is due to such effects as differing transmissivity of the sun's atmosphere at different wavelengths. A knowledge of the exact distribution of the energy constant in sunlight is important in solar cell work because these cells respond differently to different wavelengths of light.

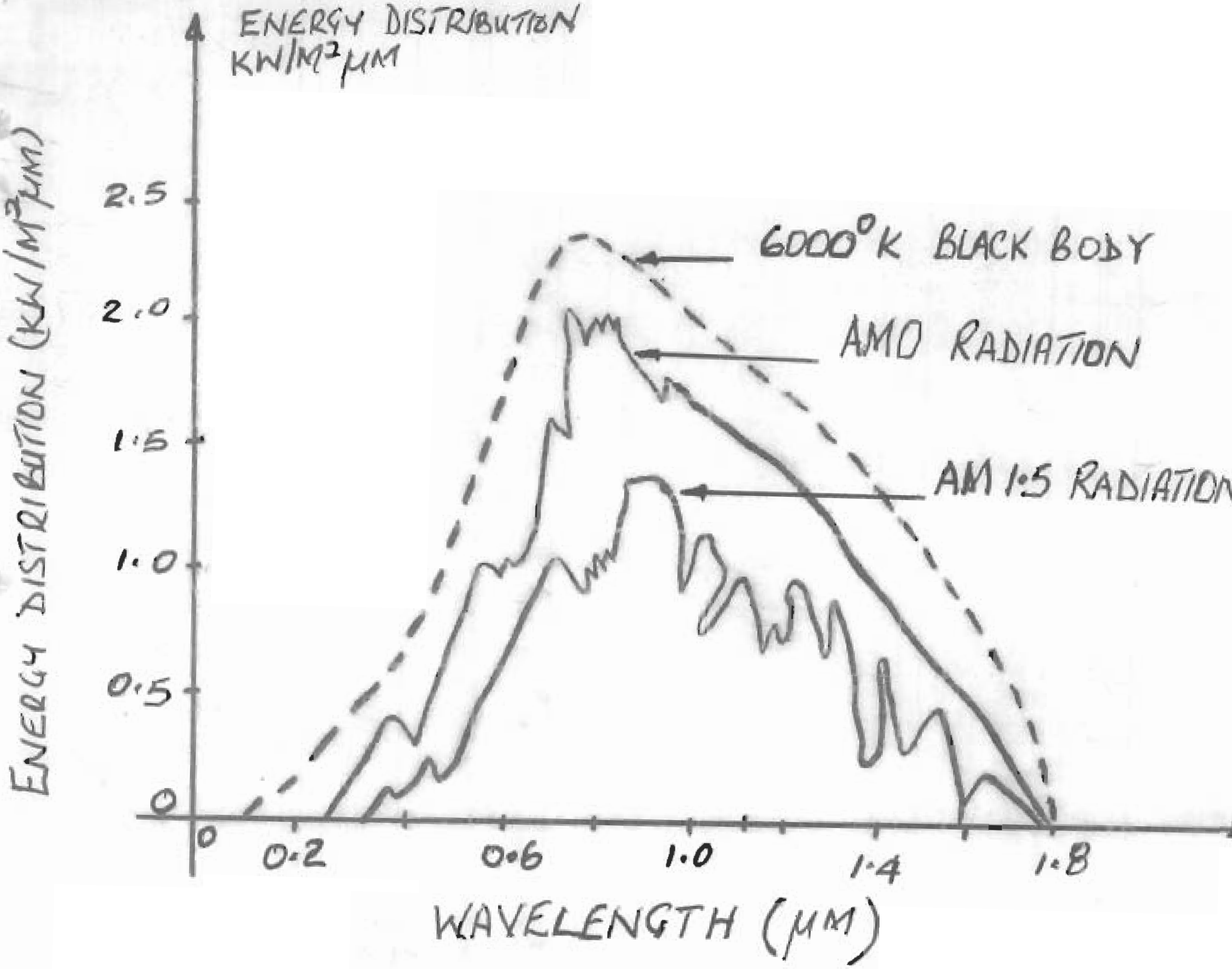

Fig. 1.0 SPECTRAL DISTRIBUTION OF SUNLIGHT

Shown are the cases of AMO and AM 1.5 radiation together with the radiation distribution expected from the sun if it were a black body at 6000°K.

During the year this solar constant can very by I 3.4%, partly due to variations in the earth-sun distance.

1.3.5 SPECTRAL DISTRIBUTION OF EXTRA TERRESTRIAL SOLAR RADIATION

The solar constant whose value is 1353 W M^{-2} is not monochromatic; it is an integral overall wavelengths from about 0.115um to about 1000um. The extra terrestrial solar spectrum consists of the ultra-violet region from 0.405 to 0.740um and the infra red from 0.740 to 1000um. The peak intensity of the extra terrestrial solar radiation occurs in the visible region at a wavelength of about 0.45um. The spectral irradiance from different wavelength intervals as well as the respective percentage of the extra terrestrial solar radiation are shown in table 1.0.

TABLE 1.0

Wavelength Range	Total Spectral Irradiance ($WM^{-2}um^{-1}$)	Percentage of Solar Constant
Ultra - Violet		
(0.115 - 0.405)	125 . 7366	9 . 293
Visible		
(0.405 - 0.740)	561 . 1724	41 . 476
Infra - Red		
0.740 - 2.000	578 . 0000	42 . 720
2.000 - 5.000	81 . 0000	6 . 023
5.000 - 10000	6 . 6000	0 . 488

Table 1.0: Extra terrestrial solar spectral.

Irradiance for Different Wavelength Ranges and their Respective Percentage (based on Solar Constant of 1353 W M^{-2}). Intensity outside the range 0.115 - 1000UM have been assumed negligible.

A more detailed tabulation of the standard solar spectrum has been published by Thekaekara[1]. The summary of their publication over the spectral distribution of extra terrestrial solar is shown below.

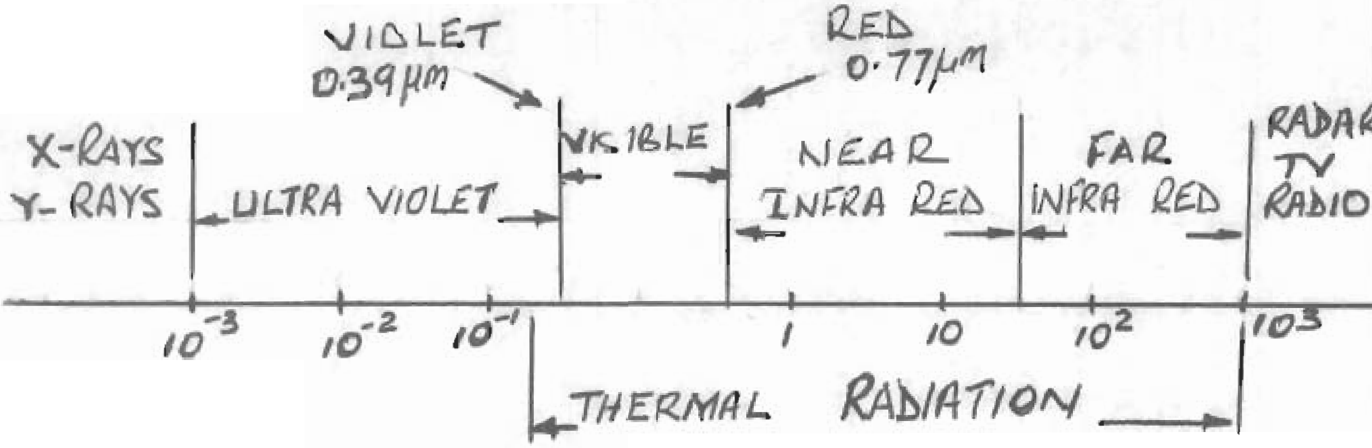

Fig. 1.1 - Spectrum of Electromagnetic Radiation

Thermal radiation wavelengths range from 0.2 - 1000μM

1UM = 10^{-6}M, angstrom 1A° = 10^{-10}M = 10^{-4}μM

Visible Spectrum - within 0.39 - 0.77μM

Ultra Violet Spectrum: 3 bands

near UV, 0.3 - 0.4μM

far UV, 0.2 - 0.3μM

max. UV, 0.00 - 0.2μM

Infra - Red Spectrum: 2 bands

near Ir, 0.77 - 25μM

far Ir, 25μM - 1000μM

1.3.6 TERRESTRIAL BEAN INSOLATION

The beam component of the terrestrial solar radiation is the result of attenuation of the extra terrestrial solar radiation. This attenuation is due to absorption and scattering by different atmospheric constituents, namely; ozone, water vapour, aerosols and carbon dioxide and dust.

The different absorbing species do not absorb at the same wavelength, nor is the absorption uniform across the entire solar spectrum. There is almost total absorption of solar energy by ozone at wavelengths below 0.3UM and by carbon dioxide at wavelength beyond 2.5UM. As a result of this the spectrum of insolation received at the earth's surface lies practically between the limits of 0.3 and 3.0UM. Even within these limits, the selective absorption by some of the atmospheric constituents (especially water vapour and carbon dioxide) drastically depletes the terrestrial beam insolation of certain wavelengths. For instance, at a wavelength of 1.384M, the solar irradiance under air mass one (AM1) condition is only 5.7W $M^{-2}UM^{-1}$ when the atmospheric turbidity β is 0.085; water vapour content is 20MM and ozone is 3.4mm.

The intra-atmospheric attenuation of the beam solar radiation is usually described quantitatively by a Beer's[2] law model as $E_{b,} = E_{o,\lambda} e^{-c\lambda m}$ ----------(12)

where $E_{b,\lambda}$ is the beam irradiance on a terrestrial surface at wavelength λ, C is the attenuation coefficient and M is the air mass (defined as the ratio of the part length of radiation through the atmospher at any given angle to the sea level path, straight through the atmosphere (vertically).

The value of the air mass depends on the altitude, Z, of the location above sea level and on the solar altitude θ, and is given by $M(Z,\theta) = M(0,\theta) \frac{P(Z)}{P(0)}$---------(13)

where P(Z) is the atmospheric pressure at the altitude Z and P(O) is the pressure at sea level, and M(0,θ) is the air mass at sea level given by

$$M(0,\theta) = \left[1229 + (614\ \mathrm{Sin})^2\right]^{\frac{1}{2}} - 614\ \mathrm{Sin}\ \theta \quad ---(14)$$

The attenuation conefficient, C includes Rayleigh attenuation coefficient C_1 (which accounts for Rayleigh Scattering), ozone absorption coefficient C_2, and absorption coefficient C_3 due to atmospheric turbidity and aerosols, this is given by

$$C_3 = \frac{\beta}{\lambda^U} \quad --------------(15)$$

where β is the turbidity coefficient and U is the wavelength exponent, large values of β and small values of U characterise highly turbid (polluted) atmosphere.

The predicominant role played by water vapour in the absorption of solar radiation is emphasised by Majumdar et al[3] in their model for the direct solar radiation. It is demonstrated in thier work that the mean absorption by water vapour content, W over a complete band varies nearly as $(W)^{0.5}$. In this model the direct solar radiation E is given by

$$E = E_e t^m\ (tw)\ \left[Wmr\right]^q \quad ----------(16)$$

where E_e is the effective radiation intensity above the tro posphere (which is a few per cent less than the solar constant), t is the transmission coefficient due to the constituents of the lower atmosphere other than water vapour, t_w is the transmission coefficient of water vapour, m is the absolute air mass (equation 9) and M_r is the relative air mass (equation 10), q = 0.5 (approximately).

The instantaneous monochromatic beam solar radiation defined in equation (7) may also be expressed in terms of the monochromatic direct transmittance, t (defined as the ratio of terrestrial beam radiation to extra terrestrial beam radiation), viz:

$$E_{b,\lambda} = t_{\lambda} \; E_{o,\lambda} \quad \text{----------(17)}$$

The transmittance consists of the absorption transmittance t_{abs}, and the scattering transmittance, t_{scat}. These are related in the following way:

$$t_{\lambda} = t_{scat,\lambda} - t_{abs.,\lambda}$$

Two types of scattering may further be distinguished. These are Rayleigh scattering due to small air molecules and scattering due to aerosols. King and Buckius[4] expressed the scattering of a monochromatic solar radiation of wavelength due to small air molecules (i.e Rayleigh scattering) as

$$T_{scat,\lambda,R} = \exp\left[-0.0089M(P/P_o)\lambda^{-4}\right] - \text{----(18)}$$

The aerosol scattering depends on the atmospheric turbidity and on the air mass and is given by

$$t_{scat,A} = \exp\left(-m\,\beta\,\lambda^{-11}\right) \quad \text{--------(19)}$$

where β is the turbidity coefficient, its value depends on the concentration of aerosols and dust in the atmosphere. β may be evaluated from the visibility X, using the equation

$$\beta = (0.55)^{\mu}\left(\frac{3.91}{X} - 0.01162\right)\left[\frac{1.577.1.132(X-5)+1.132}{23-5}\right] \text{---(20)}$$

u is a factor which depends on the size and distribution of the aerosols; its value usually lies between 0.5 and 2.5. The absorption transmittance $t_{abs.}$ is given by

$$t_{abs.} = \sum^{\text{all bands}} \left\{ E_{\lambda i} \; A_i \; \exp\left[-\int_0^{\infty} \sigma_i\, a^{+} \; A_i \; d_H \right] \right\} \Big/ E \quad \text{---(21)}$$

where A is the band absorptance of the ith absorption band, σ is the scattering coefficient, a is the absorption coefficient H is the altitude and E is the instantaneous extra terrestrial radiation, E_λ is the irradiance at a wavelength, λ.

LIOU and SASAMORI[5] have defined the band absorptance in terms of precipitable water vapour height h and mean atmospheric pressure $\bar{P}$, as

$$A = K_3 + k_4 \log \left[h(760\ \bar{P})^{k5/k_4} + 10^{-k3/k_4} \right] \quad \text{--- (22)}$$

where k_3, k_4 and k_5 are constants.

An approximate method has been given by king and Buckius[6] in terms of measurable atmospheric parameters.

$$t_{abs} = \left[C_7 + C_8 \log (Mh + C_9) \right] \exp^{(-M.B/C_{10}M)} \quad \text{---- (23)}$$

Another model for the calculation of atmospheric transmittance which includes the effects of water vapour and other particles in the atmosphere is given by Hottel[7]. This model is defined in terms of some parameters (a_o, a_1 and k) which are functions of altitude and visibility:

$$t_{atm.} = a_o + a_1 \exp(-k\,\mathrm{Cosec}\ \theta) \quad \text{------ (24)}$$

where θ is the solar altitude.

From the foregoing, if the relevant meteorological data are available transmittance and hence the intensity of the beam radiation can be evaluated. The intensity of the beam radiation can also be measured experimentally by means of pyrheliometer. However, if the data available are for global insolation only (e.g. from pyranometer readings), the beam radiation can still be evaluated using methods of correlation. The model developed by Boes et al[8] correlates the hourly beam radiation to the hourly extra terrestrial radiation by the expression.

$$E_b = \left[a\,(K_T) \times K_T + b\,(K_T) \right] E_o \text{ ------ } (25)$$

where k_T is the hourly clearness index defined as the ratio of total terrestrial, horizontal radiation E_h to extra terrestrial, horizontal radiation $E_{o,h}$ (hs);

$$\text{ie } K_T = \frac{E_h}{E_{o,h}}$$

A similar correlation method is also available for calculating the daily terrestrial beam radiation. This model was developed by Collares - Pereira and Rabl[9]. In this model the daily terrestrial beam radiation is given by

$$\frac{\bar{E}_{b,h}}{\bar{E}_h} = -0.188 + 2.272\,\bar{K}_T - 9.473\bar{K}_T^2 + 21.856\,\bar{K}_T^3 - 14.648\,\bar{K}_T^4 \text{ -------- } (26)$$

Where $\bar{K}_T$ is the daily clearness index defined as the ratio of the daily global horizontal insolation reaching the earth to the daily extra terrestrial horizontal radiation. In equation (21) $\bar{E}_{b,h}$ is the daily terrestrial beam radiation on a horizontal surface and E_h is the extra terrestrial daily radiation received by an extra terrestrial horizontal surface.

EFFECT OF CLOUDINESS ON BEAM INSOLATION

For cloudy sky the beam insolation is reduced by an amount which depends on the degree of cloudiness of the sky. One way of reflecting the effect of cloud on the beam radiation is by introducing a factor called the relative sunshine defined as $\frac{s}{S}$

where S is the maximum sunshine duration and s is the actual daily sunshine duration. The beam radiation for a cloudy day is then given by

$$E_b = K(\frac{s}{S})\, E_c \qquad (27)$$

where E_c is the daily beam radiation under clear sky condition and K is the cloudiness coefficient which, from the work of Barbara et al[10] has a value of unity.

1.3.7 DIFFUSE SOLAR RADIATION

The diffuse solar radiation falls on a terrestrial surface from all directions and at no fixed incidence angle. It is due to scattering of solar radiation in the atmosphere. The fraction of diffuse radiation in the global radiation depends on the state of cloudiness of the sky.

For a clear sky condition, it accounts for a small percentage while for a completely cloudy sky, it is the only radiation received at the earth's surface.

Ideriah[11] has proposed that in the absence of clouds, the instantaneous diffuse radiation, J may be expressed as a fraction of the contribution of scattering to the direct radiation, thus

$$J = \phi E_{scat.} = \phi_{tscat} + E_o \quad \text{-------- (28)}$$

where ϕ is a function of the solar zenith angle θ, and is given by $\phi = 0.5 \cos^{\frac{1}{3}}\theta$ for albedo (surface reflectivity) near 0.25.

For a cloudy sky, the daily diffuse solar radiation may be obtained using the expression

$$E_d = \left(\frac{s}{S}\right) E_c + f\left(1 - \frac{s}{S}\right)(E_d - E_i) \text{------(29)}$$

where E_c is the diffuse solar radiation under clear sky condition, f is an empirical transmission coefficient whose value depends on latitude and E_d is the clear sky beam radiation. In our local environment, there are two main seasons in the year; these are the wet (rainy) season and dry (harmattan) season. During the rainy season the number of sunshine hours on a given day is usually small. This means the sky is cloudy most of the time. The terrestrial insolation in this season contains a large proportion of diffuse radiation.

The harmattan months are characterized by hazy atmosphere. In a recent work, AWACHIE and OKEKE[12] observed that during these months, the mean clearness index in Enugu is usually as low as 0.36. This means that dust haze in the atmosphere causes overcast weather conditions.

LIU and JORDAN[13] have shown that the ratio of diffuse radiation to global radiation (known as the diffuse ratio) is correlated to the clearness index. This correlation is applicable to both daily and monthly insolation. Following this Inderiah and Bamiro[14] obtained the following correlation equation for the daily diffuse ratio for Ibadan (Lat 7.43^{o}N, Long. 3.9^{o}E)

$$K_d = 1.89 - 1.67 (K_T - 11.4 K_T^2 + 28.1 K_T^3 - 18.4 K^4_T \quad \text{----------(30)}$$

for $0.28 < K_T \leq 0.75$

1.3.8 IMPORTANCE OF DIFFUSE RADIATION IN PHOTOVOLTAIC ENERGY CONVERSION

The diffuse component of the terrestrial insolation plays an important part in the performance of solar cells. This has been demonstrated by DAVE and BRASLAU[15] who used numerical computations and different atmospheric models to study the performance of solar cells. Their study shows that the contribution to the photocurrent due to the diffuse radiation increases rapidly with the increase in turbidity of the atmospheric model. It also shows that for a given atmospheric model, the contribution to the photocurrent due to diffuse insolation increases rapidly when the solar zenith angle exceeds 60°. For instance, for an atmospheric model with stratus cloud layer, more than 99.9 percent of the photocurrent generated is due to diffuse sky insolation when the solar zenith angle is greater than 60°. This observation is significant in evaluating the performance of a solar cell under local environmental conditions. For an environment that is characterized by high atmospheric tubidity, it is clear that an appreciable amount of the photo current will be due to the diffuse component of the solar radiation. Also the seasonal variation of the atmospheric turbidity in a given environment will result in a seasonal variation in the relative importance of diffuse sky radiation in the performance of a solar cell.

CHAPTER TWO

2.1 SOLAR RADIATION MEASURING INSTRUMENTS

In assessing the availability of solar energy arriving on the earth, measurement of solar radiation at some locations is essential. From the measurements, empirical models are developed to predict the availability of solar energy at other locations. The three principal solar radiation fluxes arriving on the earth are direct, global and diffuse radiations and the intruments associated with measuring these three principal solar fluxes are discussed in this chapter.

There are various types of solar radiation measuring instruments, and over years considerable confusion in the terminology applied to these instruments has been built up, with a given type of instrument being designated by different names and the same name being applied to different types of instruments. For instance an instrument measuring the total hemispherical flux of solar radiation has been variously called a Pyrheliometer, pyranometer, solarimeter, actionograph and sun shine receiver or recorder. To eliminate confusion in the terminology of solar radiometry, the International Radiation Conference, meeting at Davos, Switzerland, in 1956, agreed upon the following definitions:

i) A pyrheliometer is an instrument for measuring the intensity of direct solar radiation at normal incidence.

ii) A Pyranometer is an instrument for measuring the solar radiation received from the entire hemisphere of the sky (including both direct and diffuse insolation).

iii) A pyregeometer is an instrument for measuring the net atmospheric radiation on a horizontal upward - facing black surface at the ambient air temperature.

iv) A pyrradiometer is an instrument for measuring both solar and terrestrial radiation.

v) A net Pyrradiometer is an instrument for measuring the net flux of down ward and upward total (solar, terrestrial surface and atmospheric) radiation through a horizontal surface.

Many of the solar radiometers which are in use today are designated by the names of the individuals who invented or perfected them, or the companies which manufacture them.

2.2 RADIATION SENSORS

The heart of a radiometer (i.e an instrument that measures radiant energy whether from the sun or from any other source) is its sensor, also called detector. Detectors of the various instruments can be classified as Calorimetric, thermo mechanical, thermo electric, or photo electric.

2.2.1 THERMO ELECTRIC SENSORS

A thermo electric device consists of two dissimilar metallic wires with their ends connected. An electromotive force (emf) is developed when the two junctions are at different temperatures. The emf developed is proportional to the temperature difference and depends on the material of the two metals. Example for low - temperature applications a pair of copper - Constantan is a popular combination. The temperature of the sensor changes with the intensity of solar radiation falling on it. The change in temperature is detected by means of a thermopile or a bimetallic strip. When a thermopile is used (as in the standard Eppley pyranometer), one set of junctions is in thermal contact with a blackened surface and acts as the hot junction. The other set of junctions is terminated at a highly reflective (shiny) surface. Since most of the photous incident on this surface are reflected, the set of thermopile junctions in contact with it is always at a lower temperature than the set at the black surface. As a result of the temperature difference electric current flows in the thermopile due to the well-known see back effect. The temperature difference, and hence the thermo electric current between the junction is an increasing function of intensity of solar radiation. The current is detected by means of a galvanometer which is graduated to read the intensity of insolation.

Thermo electric sensors are of various arrangements, but in a number of solar radiation measuring instruments the thermopile is arranged in a star - shaped flat grid.

2.2.2 PHOTO ELECTRIC SENSORS

In photo electric sensors, the radiation sensor is a photo cell and the photon energy is converted to electrical energy by photo voltric process. The photo - generated current, which increases with intensity of solar radiation, is measured by means of a galvanometer which is calibrated to read the intensity of solar radiation.

The disadvantage of this type of sensor is that the photo cell does not respond to the entire solar radiation spectrum because of the energy band gap requirement of the semi conductor.

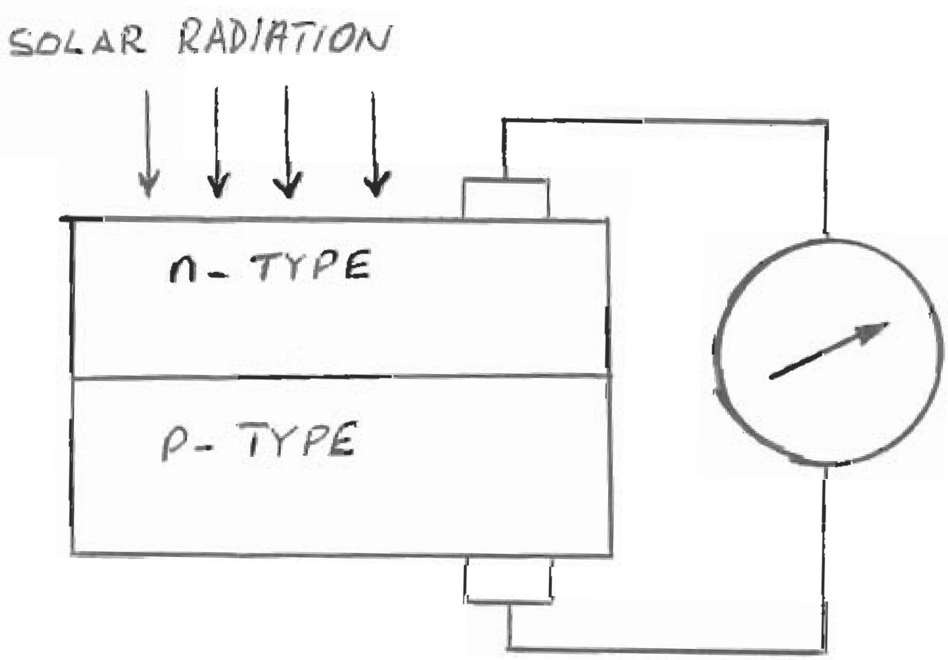

Fig 2.2 Semi Conductor p - n junction (Photo electric sensor)

2.2.3 THERMO MECHANICAL SENSORS

In the instruments based on the thermomechanical principle, the solar radiation falls on a blackened bimetallic strip. One end of the strip is fixed while the other free end is coupled to the pen of an automatic plotter via a system of levers. The fluctuation in insolation causes the temperature of the bimetallic strip to vary. The currature of the strip therefore changes with insolation; this variation in curvature is observed as a to-and-fro movement of the free end of the strip. This movement is transmitted to and magnified by the lever arrangement. The variation of the instantaneous global insolation with time.

The advantage of the thermo mechanical sensor is that it responds to all wavelengths of the solar radiation spectrum. However its accuracy in the long run may be affected by the deterioration of the black surface.

2.2.4 CALORIMETRIC SENSORS

In the calorimetric instruments, the solar radiation falls on a high-conductivity metal coated with a non-selective black paint of high absorptance. The radiant energy is then converted to heat and can be measured by various means as follows:

(i) A flowing fluid can be used to carry away the heat whose change of enthalpy is measured. The change of enthalpy then gives the incident radiant flux.

(ii) The heat gives rise to a change in the enthalpy of the absorbing metal (sensor). This increase of enthalpy (or increase in temperature) can be easily measured.

(iii) In the modern cavity - type instruments, the temperature difference across a transducer is maintained constant by additional electrical heating required between shielded and exposed phases. The irradiance is then proportional to the difference in cavity electrical heating in the two phases.

2.2.5 BOLOMETERS

This is one of the most sensitive of radiation detectors of the non selective type. Langley (1900)[16] claimed that it could register a temperature change of 0.00000001°C although this has not yet been confirmed. Its operation is based on the change of resistance of a metal on semiconductor with temperature. See fig 2.3. The two resistance elements A and B constitute two arms of a wheatstone bridge. If element A is exposed to radiation while B is shaded, the relative temperature difference which is generated between them results in an imbalance of the bridge. By proper calibration, the amount of imbalance may be interpreted in terms of the flux of radiant energy incident on the exposed element.

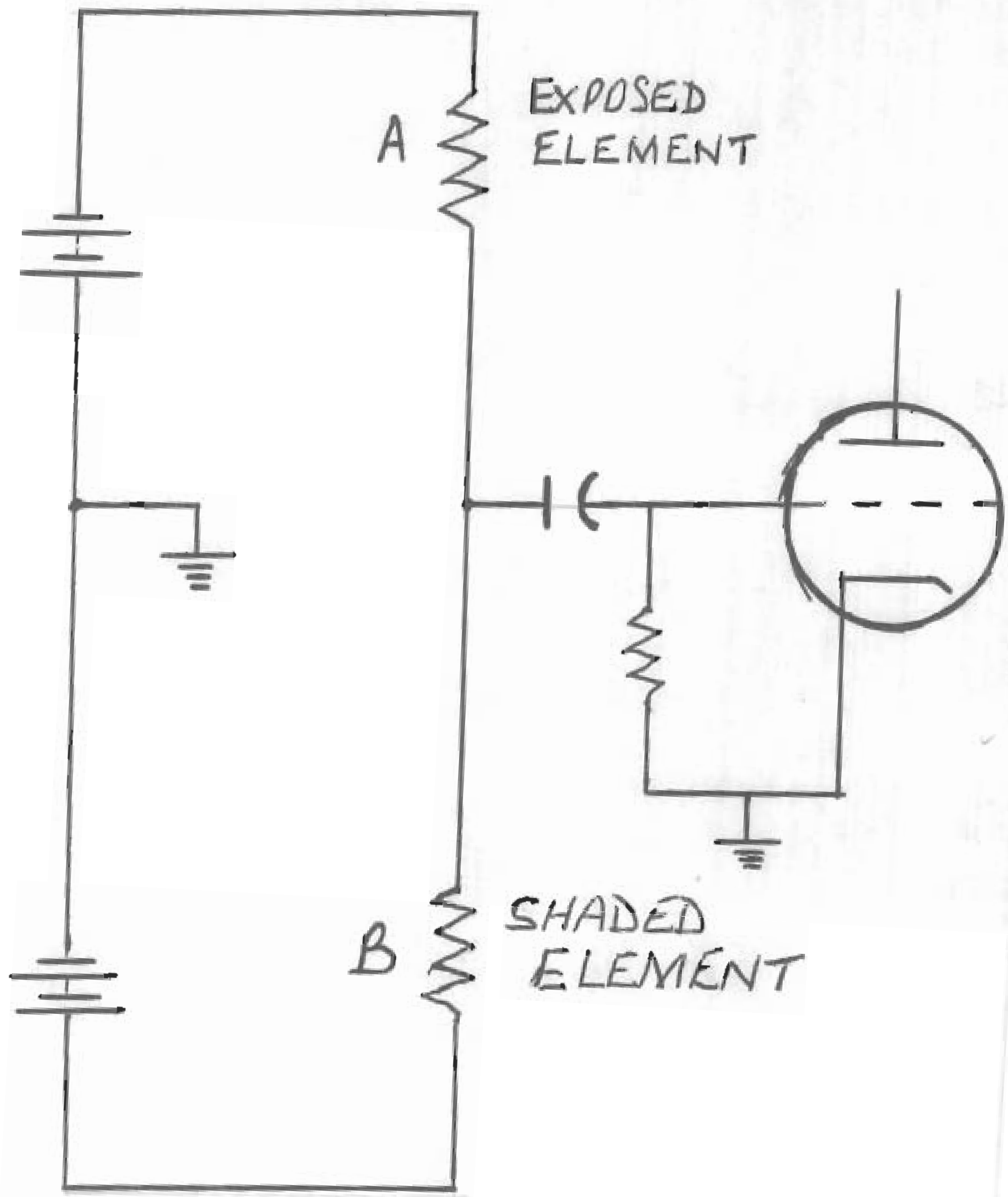

Fig. 2.3 THE ELECTRICAL CONNECTIONS OF A BOLOMETER

2.3 MEASUREMENT OF DIRECT IRRADIANCE (PYRHELIOMETERS)

2.3.1 INTRODUCTION

The first quantitative attempts to measure the intensity of the direct solar beam were begun in France by Pouillet[17] in 1838. He coined the word "pyrheliometer" from the Greek words for fire, sun and measurement. His word has now been assigned to the instrument which measures only the direct rays from the solar disk by using a collimating tube to restrict the angular acceptance of the instrument to approximately 5.7 degrees.

In a number of applications, the direct solar beam is of overwhelming importance. The direct solar beam is best measured by a normal incidence pyrheliometer mounted on a solar tracker. This instrumentation is designed for the continuous measurment of direct solar energy plus a very small amount of sky included in the field of view of the instrument; The pyrheliometer always faces the sun, and the observations made with it is called normal incidence insolation measures. This is the main advantage of this instrument.

The major problem with this instrument is the technical demand in incorporating the clock drive to enable the instrument track the sun. The daily drive has to be checked, and the instrument adjusted to accommodate seasonal changes in solar declination.

2.3.2 TYPES OF PYRHELIOMETERS

A large number of devices for measuring the direct radiation from the sun have been developed over the last 150 years or so, of which only a few are still in use. Some of the most interesting of the historical instruments are briefly discussed below.

2.3.2.1 DORNO'S PYRHELIOMETER - PHYHELIOGRAPH

One of the many devices for measuring radiation which have been developed by the Davos physical Meteorological Observantion was the pyrheliometer of C. Dorno (1922). See fig. 2.4. A blackened thermopile consisting of 18 copper - constantan thermo elements was placed in the centre of a cylindincal cavity 8mm in diameter and 24mm in length recessed into a massive 3-kg cylinder of copper. As in the Marvin and Michelson pyrheliometers, the copper provided a large heat capacity which maintained an even temperature of the inside cavity and decreased parturbations from the environment. The walls of the cavity in front of the thermpile were polished to reflect stray radiation to the blackened thermopile surface, while the rear portion of the carvity was itself blackened to absorb radiation which by-passed the thermopile. Radiation entered the instrument through a quartz lens of 20mm in diameter and 86mm in focal length. The receiving surface of the thermopile was 2.8mm behind the focal point of the lens. By use of exchangeable diaphragrms at the focal plane three different acceptance apertures could be obtained. The smallest of these was only about three quarters of a degree in angular diameter which means that only about 8 are minutes of sky around the edge of the solar disk was seen by the instrument. The other two diaphragms gave angular apertures of about 1.1° and 2.1°. Even the largest of these apertures is much smaller than the apertures of the most popular pyrheliometers in present use - Abbot Silver disk and Eppley. 5.7° Cone, Kipp and Zoneni: 10.2° Cone, Angstrom: 3 x 6° to 6 x 24° rectangle. Thus measurements from the Dorno instrument would be less subject to errors arising from scattered light in the circumsolar zone of the sky, but high - precision tracking of the sun was required.

Although the Dorno pyrheliometer appears to have incorporated some superior features, it was never widely accepted and it has been completely superseded by other types of instruments.

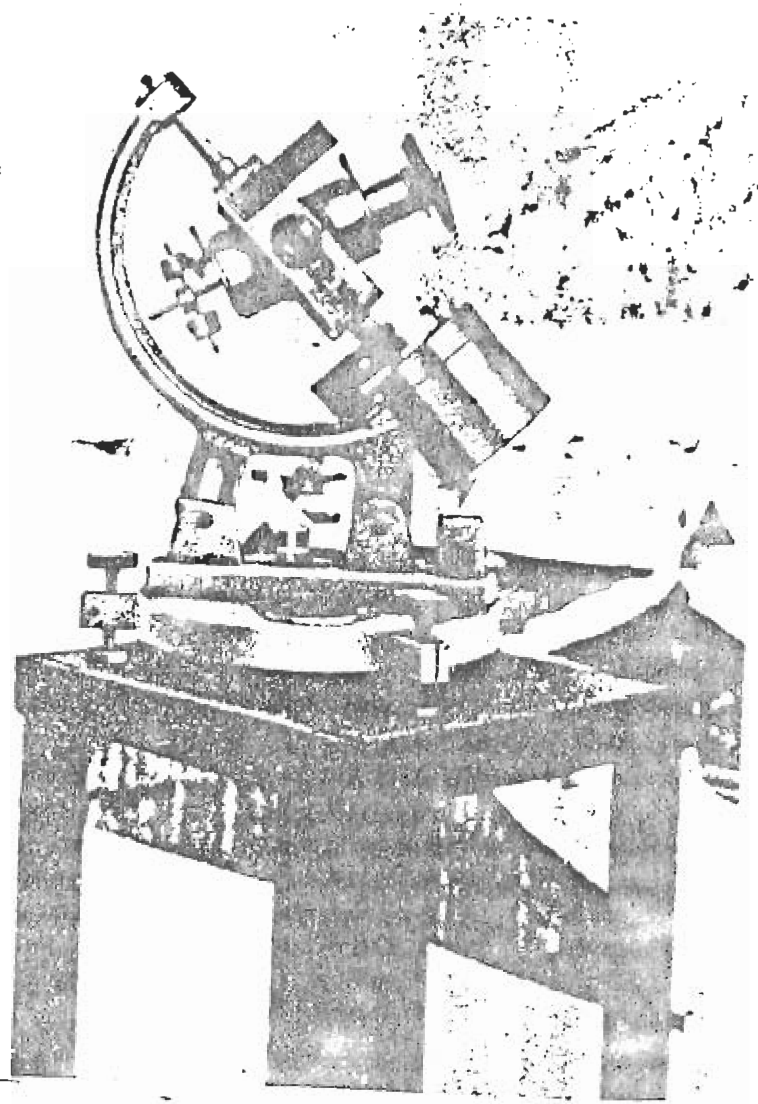

Fig. 2.4 The pyrheliometer of C. Dorno developed at the Physical-Meteorological Observatory, Davos, Switzerland (after Dorno, 1922).

2.3.2.2 VIOLLE'S PYRHELIOMETER (ACTINOMETER)

This instrument consisted of a thermometer bulb mounted in the centre of a double-walled sphere, the sp ace between the walls being filled with a constant temperature ice water bath. The thermometer bulb was shaded or exposed to the solar beam by the operation of a shutter which closed or opened the instrument aperture. In operation, the shutter was closed until an equilibrium temperature was obtained. Then the shutter was opened and the rate of rise of temperature measured. By knowing the heat capacity of the termometer bulb, the rate of energy absorption could be computed.

2.3.2.3 MARVIN PYRHELIOMETER

The design of the Marvin pyrheliometer is in many respects similar to that of the Smithsonia Abbot Silver-disk pyrheliometer. The sensing element in both cases is a blackened silver disk and the method of operation is essentially the same. The main difference between the two is that the mercury thermometer of the Smithsonian instrument is replaced in the Marvin pyrheliometer by a resistance wire for temperature sensing.

The configuration of the Marvin pyrheliometer can be seen from the picture of fig. 2.5. The sensing element was a disk of blackened silver 4.5cm in diameter and 0.3cm in thickness, which is suspended by three fine wires in a metal support encased in the spherical wooden shell which formed the base of the instrument. The wood of the shell protected the disk from short period changes of the ambient environemnt. Radiation was admitted to the instrument through a collimator tube fitted with optical diaphragms, and blackened inside, and the instrument was pointed at the sun by a clock-driven equatorial mount. An electrically operated shutter mounted in front of the entrance aperture caused alternate 1-mm intervals of shading exposure of the blackened surface of the disk. The Marvin instrument is now completely obsolete. See fig. 2.5.

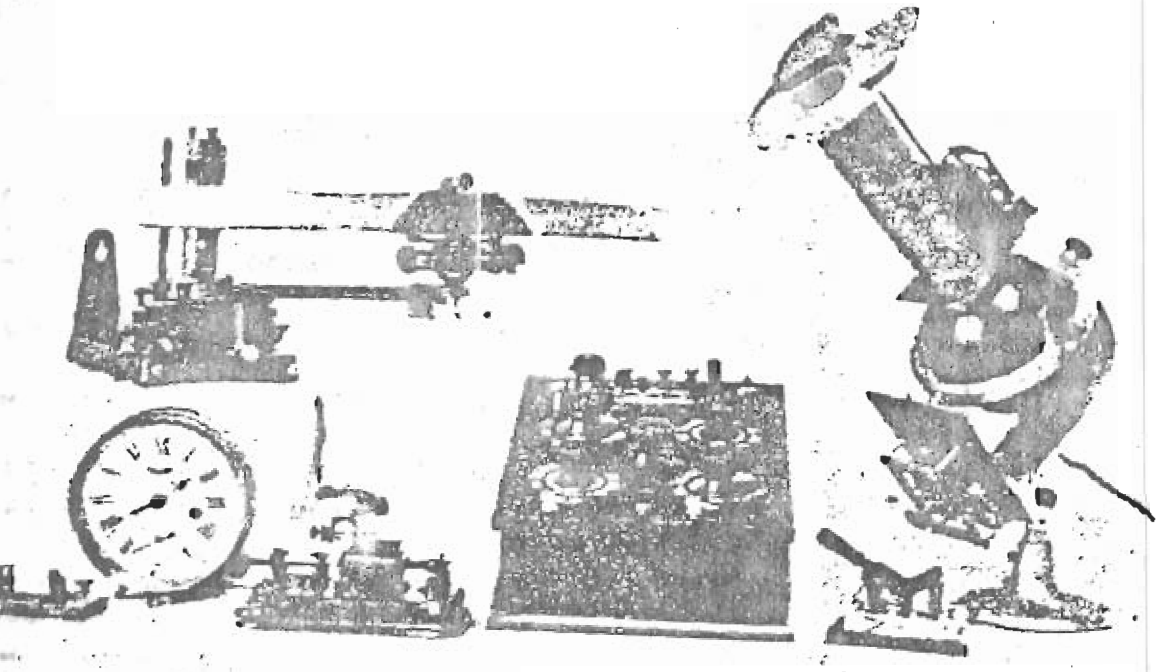

Fig. 2.5 The Marvin pyrheliometer (far right) with various accessories used in [me]asuring the flux of direct solar radiation (after Covert, 1925).

2.3.2.4 HERSCHEL'S PYRHELIOMETER (ACTINOMETER)

Herschels's Actionometer developed about 1825, was one of the first instruments used for measuring the heating effect of direct solar radiation and it was the first in which the rate of coding was introduced into solar radiation measurement. This instrument consisted of a thermometer with a large cylindrical glass bulb filled with a liquid which was coloured deep blue to promote absorption of solar radiation. In operation, the thermometer bulb was shaded from direct sunlight for 1 minute, then exposed for 1 minute, and again shaded 1 minute. The thermometer readings obtained during this three - stage circle could, on calibration by a known energy source, be interpreted in terms of the direct solar energy on the instrument. The method of making radiation determinations by alternately shading and exposing the sensor was adopted in many of the later instrument.

2.3.2.5 HODGKINSON'S PYRHELIOMETER (ACTINOMETER)

The principle of this instrument is the same as that of Herschel's actinometer, but it was made lighter and more steady for use in the mountains. It had 2.5cm diameter thermometer bulb fitted with alcohol coloured with aniline blue.

This bulb was mounted in the middle of a bright metal tube of about 6cm in diameter and 45cm in length, the ends of which were covered by caps of clear plate glass. The stem of the thermometer projected through a hole in the wall of the tube. As with Herchel's actinometer, the reading of the thermometer after a series of alternate intervals of shading and exposure of the bulb, was used (after calibration) to determine the flux of solar radiation.

2.3.2.6 POUILLET'S PYRHELIOMETER

The first successful research on the solar constant appears to have been that of pouillet[18] in 1837 (Glaze Brook 1923). His instruments radiation receiver was a flat cylindrical vessel which was filled with water (mercury at a later stage), and act as a calirmeter. The exposed face of the cylinder was blackened to provide an absorbent surface, while the other surface of the cylinder was silvered to decrease radiative exchange. A thermometer bulb was sealed into the liquid of the cylinder, and the stem of the thermometer extended along the axis. Rotation of the cylinder around the axis mixed the liquid to provide more representative temperature measurements.

In operation, the blackened face of the receiver was directed to a part of the sky, away from the sun for a period of 5 minutes, and the fall of temperature was noted. During the next 5 minutes the black surface was exposed normally to the solar beam, and the rise of temperature noted. Finally, the receiving surface was again directed away from the sun for 5 minutes and the fall of temperature was noted. From a knowledge of the heat capacity of the calorimeter, the total heat received per unit surface and unit time could be computed. Pouillet[19] obtained a value (1.7 cal $cm^{-2}min^{-1}$) of the solar constant which was within 14% of our present most generally accepted value (1.94 cal $cm^{-2}min^{-1}$).

2.3.3 CLASSIFICATION OF PYRHELIOMETERS

There are many types of commercially available pyrheliometer. These are classified by the commission for instruments and Methods of Observation of the World Meteorological Organisation (WMO) in 1965 as standard, first class and second class, in accordance with the criteria given in Table 2.1.

TABLE 2.1

CLASSIFICATION OF PYRHELIOMETERS

	STANDARD	IST CLASS	2ND CLASS
Sensitivity (MWCM^{-2})	± 0.20	±0.40	±0.50
Stability (% change per year)	± 0.20	±1.00	±2.00
Temperature (Maximum error due to changes of ambient temperature %)	± 0.20	±1.00	±2.00
Selectivity (Maximum error due to departure from assumed spectral responses %)	± 1.00	±1.00	±2.00
Lineavity (Maximum error due to non-lineavity not accounted for %)	± 0.50	±1.00	±2.00
Time Constant (Maximum)	25.00S	25.00S	60.00S

Some available Pyrheliometers are described below as typical examples of standard or first class or second class pyrheliometer.

2.3.3.1 ANGSTROM ELECTRICAL COMPENSATION PYRHELIOMETER

This is about the first reliable pyrheliometer and one of the most accurate, as well as convenient instruments for measuring radiant energies. It consists of two strips of manganin foil of approximate dimensions 20 X 2 X 0.01 mm coated on one side with parson's optical black lacquer. The strips are mounted side by side across the opening of the strip holder as shown in figure 2.5. A thermo junction is attached to the back side of each strip, and electrical leads from the strips and the thermo junctions are attached to external binding posts on the base of the holder. The holder is mounted at the base of a cylindrical metal tube T (shown in fig 2.6) which is itself attached to an azimuth - elevation mechanism by which the tube can be directed at the sun A reversible shutter at the front end of the tube permits one of the strips to be shaded from the sun, while the other is exposed to the direct solar radiation.

In operation, the shaded strip is heated by an electric current to the same temperature as that of the exposed strip, at which time the rate of energy absorption by the exposed strip is thermo-electrically compensated by the rate of energy supplied electrically to the shaded strip. Equivalent temperature of the strips is determined by the thermo junctions attached to their reverse sides, being connected in opposition through a sensitive null detector.

With regards to the construction of the instrument, most of the earlier models suffered from the so - called "edge effect" caused by the exposed strip being shaded at the ends by the innermost diaphragm while the shaded and electrically heated strip has the same temperature over its whole length. It is estimated that this introduced an error of the order of - 2.0%. In recent designs, this effect is largely eliminated through arranging for the screening to occur exactly at the terminations of the strip. Other possible sources of error arise from the inability to heat the shaded strip in the same manner as the exposed one, and from differences in the thermal conductance of the strip blackening. Finally, small optical effects may be introduced within the diaphragm system of the pyrheliometer tube and behind the strips.

Although the Angstrom instrument is normally calibrated against a Primary standard, it has the capability in itself of absolute energy determination. It is rated as a standard instrument by the World Meteorological Organisation (WMO).

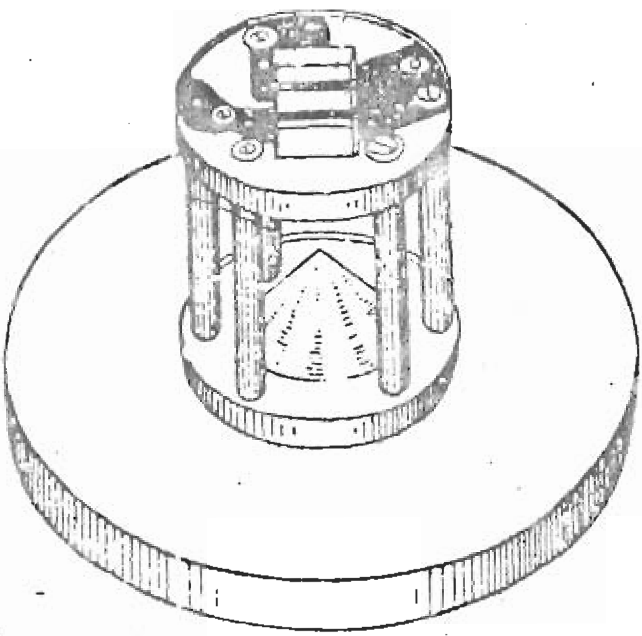

Fig. 2.6 The base of the Ångström electrical compensation pyrheliometer showing the blackened receiving strips (after K. Ångström, 1899).

Fig. 2.7 A traditional model of the Ångström electrical compensation pyrheliometer (photograph from Science Museum, London).

2.3.3.2 ABBOT SILVER - DISK PYRHELIOMETER

The Silver - disk pyrheliometer was introduced originally as a secondary instrument by the Smithsonian Institution; although it is mainly used now as a transfer standard for calibrating other radiation instruments. The design of the instrument is shown in figure 2.6.

It has a sensitive element of a blackened Silver disk, D of dimension 38 mm in diameter and 7 mm in thickness. The disk has a hole bored radially into its edge, into which is inserted the bulb of a sensitive mercury - in - glass thermometer T. The space surrounding the thermometer bub bulb is filled with mercury in order to promote a rapid transfer of heat between the Silver disk and the thermometer. A thin steel lining in the hole prevents amalgamation of the mercury and silver. Finally, the mercury is kept from escaping from the hole by a seal of cord, shellac, and wax surrounding the thermometer stem. The disk is suspended by three fine steel wires inside a copper box B, which is enclosed in a wooden box to protect the instrument from temperature changes of the surroundings - see fig. 2.8.

In operation, solar radiation enters the instrument through the Collimator tube labelled C in figure 2.8, and is absorbed by the blackened silver disk, D and causes a rise in temperature of the disk. The rate of change of temperature of the disk monitored by careful monitoring of the the thermometer readings in a series of 2 minutes cycles. The

The field of view of the instrument is limited (by appropriate diaphragms inside the collimator tube) to a circular cone of hole aperture angle of 5.7°. The thermometer stem is bent at a right angle to make the instrument more compact and easier to use. It is graduated in tenths of degree celsius from - 15° to 50°C, and the readings are made to hundredths of a degree.

A three - wafer shutter of polished metal plates is rotated in and out of the field of view to alternately shade and expose the silver disk to solar radiation in a specified and carefully timed sequence. After the temperature readings obtained during the sequence are connected for air, stem and bulb temperatures, the final values of energy flux are obtained by multiplying the corrected temperature difference by a calibration Constant for the particular instrument being used.

The instrument is rated as a standard instrument by the World Meteorological Organisation (WMO).

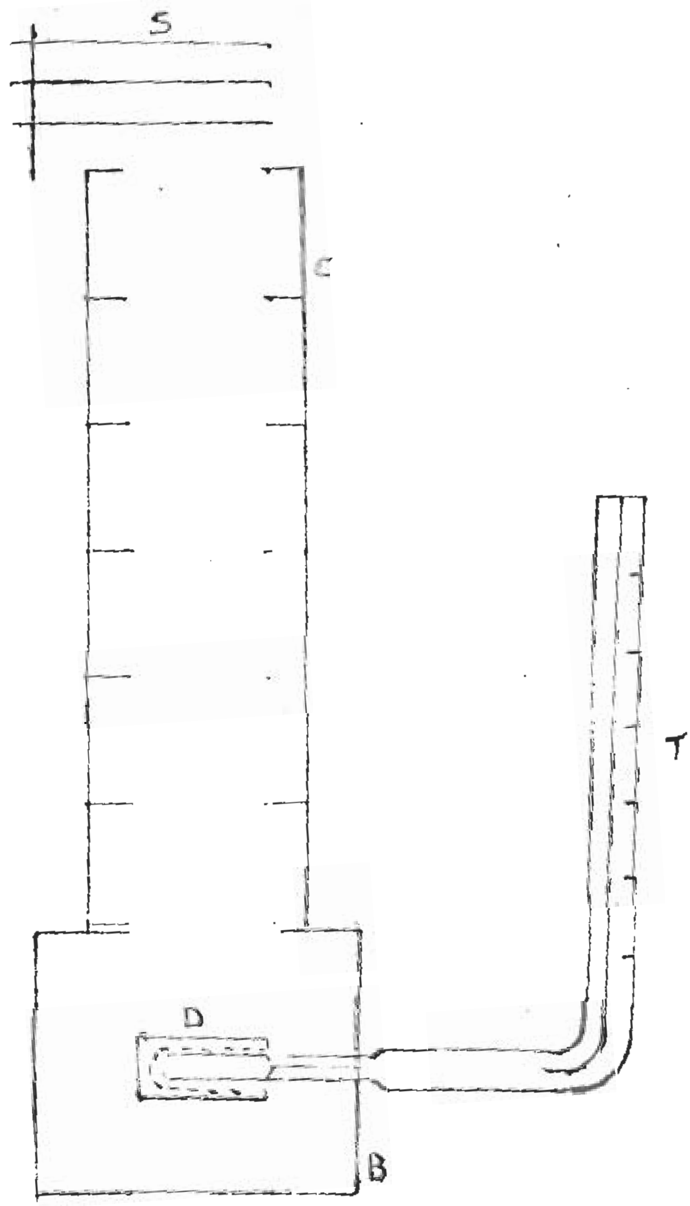

Fig. 2.8 SCHEMATIC DIAGRAM OF THE SILVER-DISK PYRHELIOMETER. S, SHUTTER; C, COLLIMATOR TUBE; D, BLACKENED SILVER DISK; B, COPPER BLOCK; T, THERMOMETER.

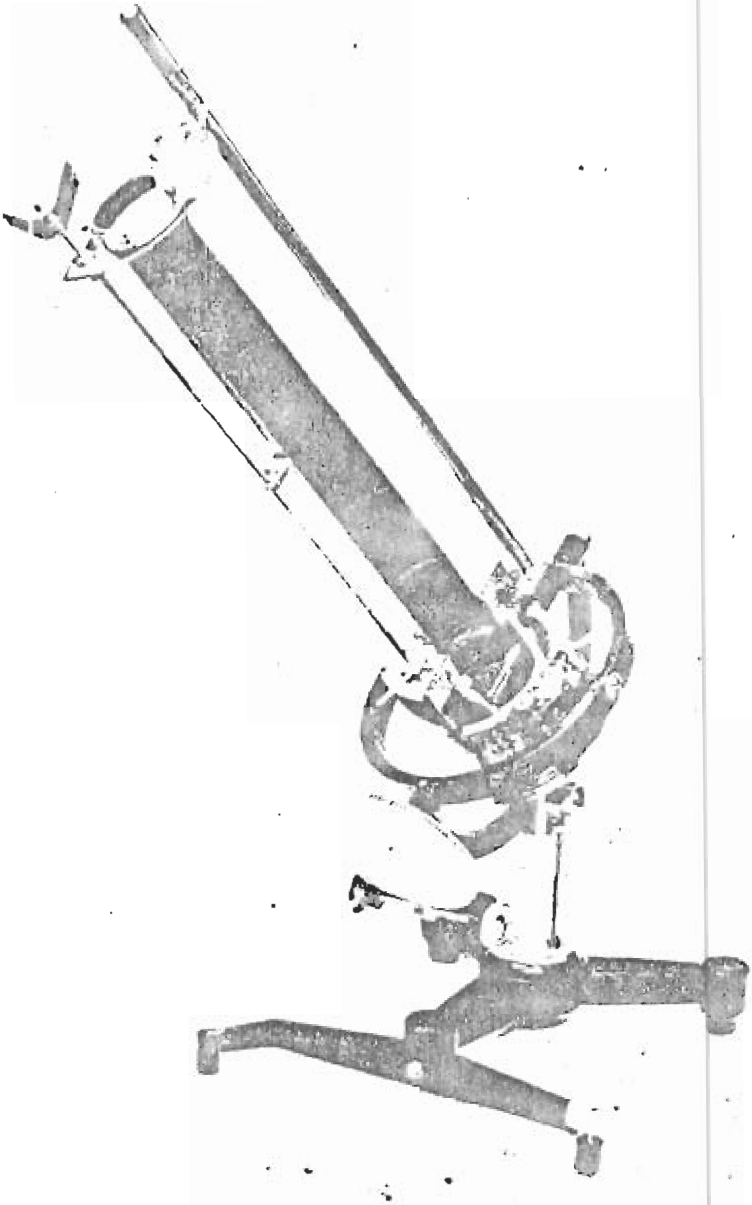

Fig. 2.9 Photo of the silver-disk pyrheliometer with a section removed to reveal the silver disk and inserted thermometer (courtesy of the Smithsonian Institution).

2.3.3.3 EPPLEY NORMAL INCIDENCE PYRHELIOMETER

This instrument in its present form, has a sensitive element of a fast - response wire-wound plated (copper-constantan) multijunction thermopile with a 9mm diameter receiver coated with Parson's optical black Lacquer. A temperature compensating circuit to stabilize sensor response is incorporated in the heat sink of the thermopile. The unit is mounted at the base of a double-walled brass tube which is chromed externally and blackened internally. A series of diaphragms limits the aperture to a circular cone of full angle 5.7°. The inner-most diaphragm screens a 1mm anulus of the receiver at its edge; this reduces the sensitivity from perfect solar tracking. The arrangement of an air-insulated double-walled cover significantly increases instrument stability especially in windy conditions. The interior of the system is filled with dry air at atmospheric pressure, and the viewing end is sealed by a removable insert carrying a crystal quartz window of 1mm thickness. Two flanges, one at each end of the pyrheliometer tube are provided with sighting devices to allow the instrument to be oriented towards the sun. A normally rotable disk, which can accommodate three filters and leave one aperture for total spectrum measurements is provided - see fig. 2.10.

The sensitivity of the instrument is 5 - 6 mV/cal CM^2 min with an impedence of 200Ω approximately. It has a temperature dependence of ±1% over a range of - 30° to 40°C and a linearity of response which is linear up to 4Cal $CM^{-2}min^{-1}$ Its response is suitable for remote recording and the case is weather proofed for continuous operation in an exposed location. In practice, the instrument is normally attached to an electrically driven equatorial mount for solar tracking and the output signal is either recorded directly on a strip - chart Recorder or integrated over an appropriate time period and registered.

By occasional re-standardization, the instrument can be used as a secondary standard for calibrating other pyrheliometers.

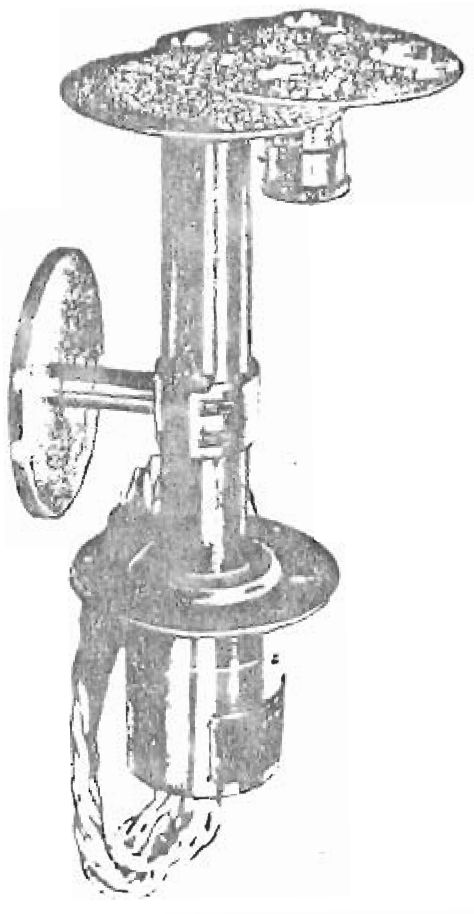

Fig.2.10 The Eppley normal incidence pyrheliometer (courtesy of the Eppley Laboratories).

2.3.3.4 MICHELSON BIMETALLIC PYRHELIOMETER

This pyrheliometer was orginally constructed in Moscow at about the same time as the Abbot-Silver disk Pyrheliometer. It is in reality, a bimetallic thermometer as shown in fig. 2.11.

In principle, the deflection of a delicate fibre I attached to the free end of a fine bimetallic (usually constantan - Invar) blackened lamina S, irradiated by the solar beam A, is observed through a relatively low power microscope M. The aperture of the instrument has angles of approximately 5^o and 13^o. It is of reasonably rapid response (20 - 30 sec. for a 100% intensity change).

On account of its portability, the bimetallic pyrheliometer is especially suitable for use as an instrument for daily routine measurements and also as a travelling substandard in a radiation network. It can be equipped with a quartz window and interchangeable filters. Use of the window is advantageous in windy conditions, and with the recommended filters, measurements of atmospheric turbidity are readily obtainable. However, the fragile nature of the instrument and the need for frequent re-calibration, for standardising purposes, results in its limited popularity.

The calibrated factor must be determined by comparism with another well - calibrated pyrheliometer. It is expressed as the caloric value of one scale unit. In principle, the

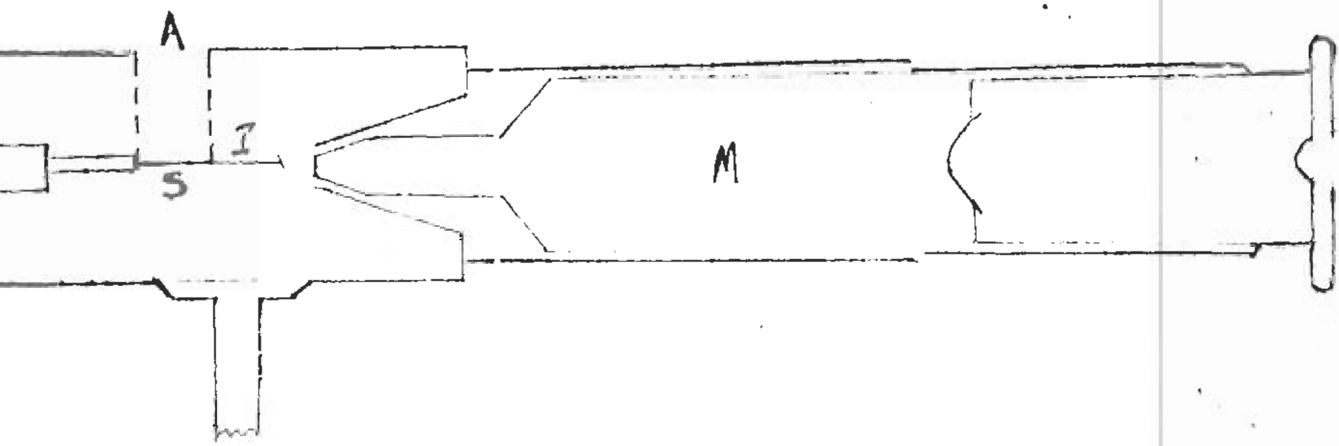

Fig. 2.11 SIMPLIFIED DIAGRAM OF THE MICHELSON
IMETALIC PYRHELIOMETER. A, APERTURE; S, BLACKENED
AMINA; I, FIBER; M, MICROSCOPE.

calibration factor of this bimetallic instrument has a dependence on the instrument temperature which has to be determined experimentally. This temperature dependence has to be taken into consideration for routine measurements as well as for calibration. It is rated as first class pyrheliometer by the World Meteorological Organisation (WMO).

2.3.3.5 SAVINOV - YANISHEVSKY PYRHELIOMETER - ACTINOMETER

This is the main operational pyrheliometer for direct solar radiation measurement in the U.S.S.R. It is used as a relative instrument, and therefore requires calibration against an absolute standard. The primary standard in the U.S.S.R is the Angstrom electrical compensation pyrheliometer.

The sensor in this instrument is a thin blackened silver disk, 11 mm in diameter, from which the centre section of 3.5 mm diameter has been removed. To the back of the disk are cemented the hot junctions of 36 pairs of thermopile made from 6.0 X 0.3 X 0.04 mm strips of manganin and constantan. The cold junction are cemented to a heavy copper ring, which is in good thermal contact with the main body of the instrument. The radial orientation of the thermopile has given rise to the designation "thermostar" (thermozvezdockkoi) for the sensor assembly - see fig. 2.12.

The thermoster is mounted at the bottom of a collimator tube, the aperture of which is a 5.0° circular cone. Conductors from the thermostar are led out from the base of the instrument to an indicator or recorder, the main recorders in use being the galvanometric or balancing potentio-metric type. The internal resistance of the thermostar is 15 - 20 Ohms and the output signal is

4 - 7mV for an incident flux of 1.0 cal CM^{-2} min^{-1}. The response of the instrument is approximately proportional to the flux of incidence solar radiation. The instrument is not temperature compensated, the temperature dependence being about - 0.1% rise in ambient temperature. It is used for continuous measurements of direct solar radiation by being installed on a clock - driven equatorial mount.

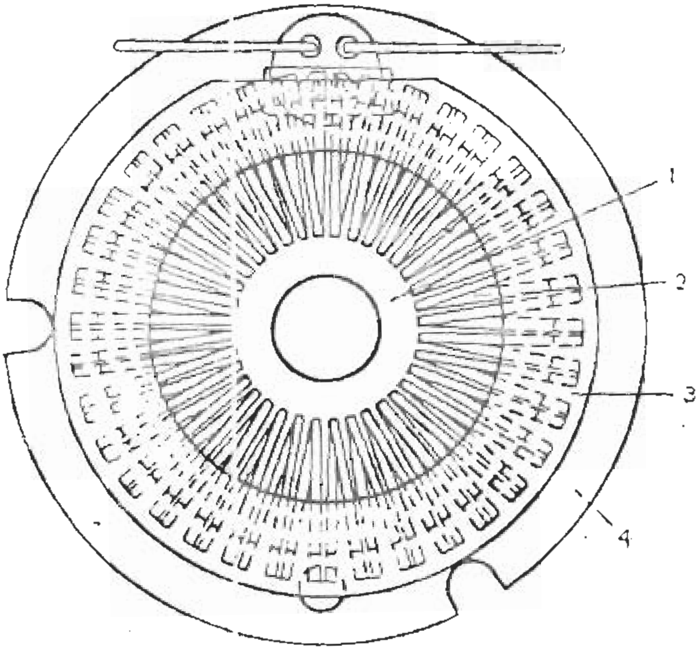

Fig. 2.12 Diagram showing the thermocouple arrangement (the "thermostar")
of the Savinov-Yanishevsky pyrheliometer (after Yanishevsky, 1957).

2.3.4 CALIBRATION OF PYRHELIOMETERS

Pyrheliometers which are normally used as operational instruments including the Eppley, Linke - Feussner, Savinov Yanishevsky and other recording types, are not designed to be absolute instruments, so they require calibration against standard instruments in order that their indications may be interpreted in terms of absolute energy. The main standard pyrheliometers which have been developed are the Angstron electrical compensation and the Smithsonian water - flow pyrheliometers. The water - flow pyrheliometer is somewhat complicated and difficult to use; thus this leaves the Angstron pyrheliometer as the primary standard to which other solar radiation instruments are referenced.

Working standard pyrheliometers of the Angstron type are maintained at regional and national centres designated by the world Meteorological Organisation for the purpose of reproducing the International Pyrheliometric scale 1956(IPS). To a limited extent, the Abbot Silver-disk pyrheliometer is still employed at such centres. The secondary transfer instruments in current use are other Angstron pyrheliometer and instruments of the Eppley, Linke - Feussner and Michelson type.

Once a good secondary instrument is properly calibrated, there is little difficulty in using it to transfer this calibration to operational instruments. The comparism should be carried out when there is as little haze; smoke or other obscuring materials as possible in the atmosphere, and under conditions in which no clouds are within 20° of the sun. The two instruments should be installed in close proximity to each other on mounts by which they can easily be oriented to the sun. A sufficient number (at least ten) of comparisons should be made between the secondary standard and the operational instrument to secure a representative constant for the latter.

If $\bar{F}$ is the average flux of solar radiation determined from n readings of the secondary standard and $\bar{r}$ is the average response (in milli volts or other units) determined by an equivalent number of readings of the operational instrument, then the required constant C is given by

$$C = \frac{\bar{F}}{\bar{r}} .$$

2.4.0 MEASUREMENT OF GLOBAL IRRADIANCE (PYRANOMETERS)

The intensity of solar radiation is measured by means of a pyranometer. The pyranometer measures the global (or total) radiation (i.e diffuse plus beam) at a given location. It consists essentially of a device which can detect solar radiation (i.e a radiation sensor) enclosed by a glass dome.

The advantage of pyranometer is that it is a simple instrument requiring no tracking of the sun. The major disadvantage of pyranometer is that as it does not track the sun, it does not collect all the radiation there is from the sources, especially early morning and late evening radiations.

There are different types of pyranometer. Some of these types of pyranometers that are in early development are described below:

A. CALLENDAR PYRANOMETERS

This pyranometer, invented by an English physicist, H.S. Callendar[20], in 1898, had a sensor made up of four platinum wire grids wound on strips of mica and connected in pairs such that each pair constituted an electrical resistance thermometer. One pair of grids was coated with black enamel to promote the absorption of sun light, while the other pair was left as highly reflecting platinum metal. The grids were arranged in a checker-board configuration and mounted in an evacuated glass bulb as shown in fig. 2.13.

The difference in temperature developed between the pairs of grids on exposure to solar radiation was very nearly proportional to the intensity of the radiation incident on them. The temperature difference was recorded by connecting the two pairs of grids as Wheatstone bridge with a pen arrangement which made traces on a revolving drum. Each instrument was accompanied by a calibration factor by which the recorded temperature difference could be interpreted in terms of the flux radiant energy to which it is exposed.

The instrument had a relatively widespread use in the early 20th century, however, with the development of thermoelectric sensors, it was gradually replaced.

Fig. 2.13 Photograph of the Callendar pyranometer (copyright by The Science Museum, London; reproduced by permission).

B. ANGSTROM PYRANOMETER

The operational mode of this instrument was based on electrical compensation principle. The receiver surface consisted of two white strips (aa) which were coated with magnesium oxide and two black strips (bb) which were covered with platinum black (see fig. 2.14). The four strips were mounted side by side on an insulating frame work in the end of a nickel - plated cylinder, and thermo junctions were attached from them electrically. The white strips were connected through a sensitive milliammeter and variable resistance to a low - voltage battery. The glass hemisphere (g) was supported by the metal disk (d), into which was inserted a Vial of drying agent.

In operation, the strips were maintained at the same temperature by heat being supplied electrically to the white strips to compensate for the greater amount of radiant energy being absorbed by the black strips.

In spite of some attractive features, this instrument was never put into widespread use.

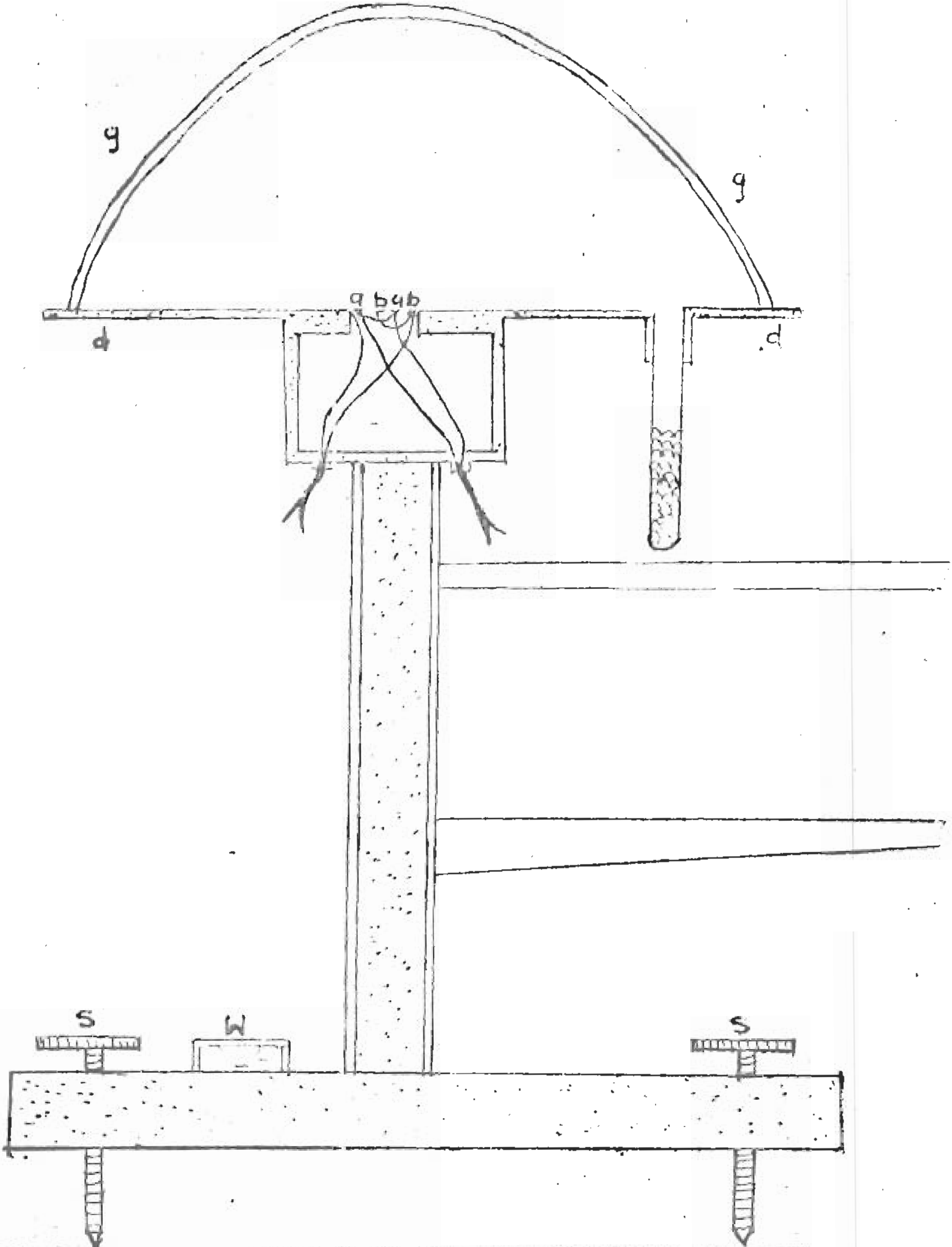

Fig.2.14 Schematic diagram of the Angs trom electr ical compensation Pyranometer

C. SMITHSONIAN PYRANOMETER

The sensor of this instrument consisted of two blackened manganin strips (a and b). Strip b was ten times as thick as strip a, and therefore had a higher heat conductance than did a. The ends of both strips were soldered to copper posts which were in good thermal contact with a nickel - plated copper block. The strips were electrically insulated, however, from the copper block and from each other by mica strips. Tellurium - platinum thermo elements were attached by waxed paper to the back of the manganin strips and were connected in series through a sensitive galvanometer so that the amount of deflection of the galvanometer indicated the difference in the temperature of the strips.

This instrument, however, was never put into general use, because of the galvanometer drifts and other problems.

2.5. MODERN PYRANOMETERS

All of the pyranometers which have been developed require calibration with respect to a primary radiation standard, so none can be classed as a standard pyranometer. On the basis of accuracy and overall system performance, World Meteorological Organisation, WMO (1965) defined three classes of pyranometers. The bases for the classification are given in table 1.3.

TABLE 2.2

CLASSIFICATION OF PYRANOMETER

	IST CLASS	2ND CLASS	3RD CLASS
Sensitivity ($MWCM^{-2}$)	±0.1	±0.5	±1.0
Stability (% change per year)	±1.0	±2.0	±5.0
Change of ambient temperature %	±1.0	±2.0	±5.0
Selectivity (Max error due to departure from assumed spectral response %)	±1.0	±2.0	±5.0
Linearity (Max. error due to non linearity not accounted for (%)	±1.0	±2.0	±3.0
Time Constant (Maximum)	25 sec	60 sec	240 s
Cosine response (deviation from the assumed, taked at sun elevation 10° on clear day %)	±3.0	±5-7.0	±10.0
Azimuth response (deviation from that assumed, taken on clear day (%)	±3.0	±5-7.0	±10.0

Some available pyranometers are:

2.5.1 EPPLEY 180^0 PYRANOMETER

This instrument has been by far the most widely used solar radiation instrument in the United States. The sensor of the instrument is a thermopile of gold - palladium and platinium - rhodium alloys, the junctions of which are in good thermal contact, but electrically insulated from the concentric rings of the disk as shown in fig. 2.15.
The disk with a total diameter of about 29 mm, is made up of two thin flat silver rings and a small inside disk, all of which are thermally insulated from each other. The outside ring and the small disk are coated with magnesium oxide, a material which has a high reflectance for radiation in the solar wavelength range. The inside ring is coated with Parson's optical black lacquer, and therefore has a low reflectance at solar wavelengths. Their different temperatures on exposure to solar radiation, causes an electromotive force to be produced between the attached thermojunction. The temperature difference between the hot and cold junctions is a function of the total amount of shortwave radiation, on the device. Therefore, by accurate calibration the voltage from the thermopile can be interpreted in terms of the incident solar energy.
To a close approximation the output voltage is a linear function of the incident energy.

The glass bulb surrounding the sensing disk was filled with dry air at atmospheric pressure at the time of manufacture. The bulb being approximately spherical, 76 mm in diameter, and made of soda lime glass of approximately 0.6 mm thickness, the effects due to selective transmission of the glass for solar wavelengths are minor. Transmission of the glass is almost constant at slightly over 0.9 between about 0.35 and 2.6 m. The instrument will respond somewhat selectively to wavelengths near the effective limits of the solar spectrum. But to the extent that the measurement conditions are similar to the conditions under which the instrument is calibrated, the spectral selectivity introduces no errors in the measurement results. For practical purposes, the effects of spectral selectivity due to the glass are negligible.

The Eppley pyranometers are subject to a significant dependance of sensitivity on ambient temperature. Sensitivity decreases with increasing temperature by between 0.05 and 0.15% per $1^{\circ}C$ rise in temperatures over a range -50° to $40^{\circ}C$. Since the normal response of thermo couples is for an increase of sensitivity with increasing temperature, it appears that the observed decrease is caused by convection inside the pyranometer bulb.

A considerable improvement in the performance of the Eppley instrument can be achieved by the insertion of a thermistor of about 2000 Ohms resistance in series with one of the thermopile leads. Since the positive temperature coefficient of the thermistor is much larger in absolute magnitude than the negative temperature coefficient of the thermopile an auxilliary shunt with about 1500 Ohms resistance is introduced into the circuit. Temperature Compensation is brought about by the decrease of resistance and a consequent decrease of potential drop in the circuit, with increasing temperature of the thermistor. The thermistor is inserted in the heat sink of the receiving element and thereby subject to the temperature of the element while being shielded from incident radiation.

The Eppley instrument is subject to an additional error associated with changing angle of incidence of the radiation on the detector. The instrument response is degraded very seriously at angles of incidence greater than about 60^{o}. The reason for the degradation is probably due to a change of reflectance of the receiving surfaces, particularly the black surface, with angle of incidence. However, improper alignment of the elements or inhomogeneities in the glass envelope may be contributory factors.

This instrument is no longer in production, although a large number of it is still in operation. It has since been replaced by other types of pyranometer viz, Eppley Black - and - white, and Eppley precision spectral pyranometers.

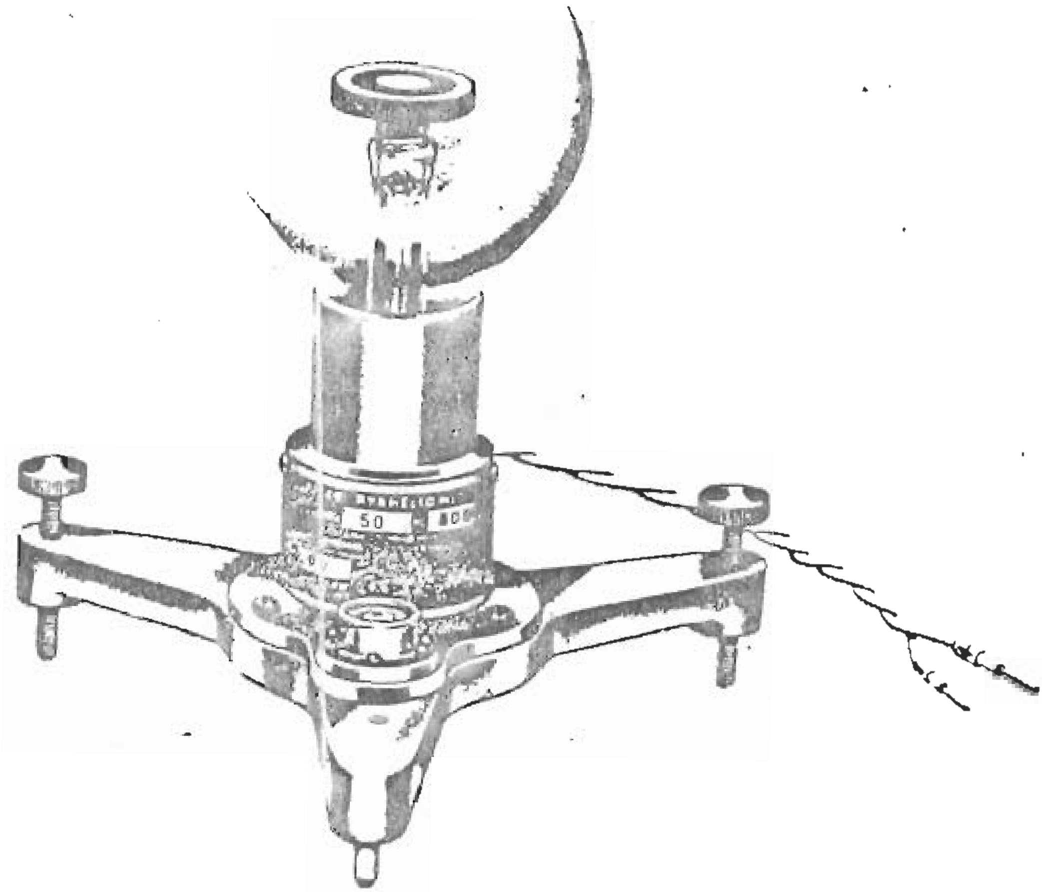

Fig. 2.15 The Eppley pyranometer which has received widespread application, particularly in the United States (courtesy of the Eppley Laboratories). This model is no longer in production.

2.5.2 EPPLEY BLACK - AND - WHITE PYRANOMETER

The detector of this instrument is a wire - wound of thermopile made by electroplating copper on constantan. The hot and cold junctions are painted with Parson's optical Black Paint and barium sulphate respectively. A built-in temperature compensation provides a signal which is independent of temperature to within ± 1.5% from -20° to $40^{\circ}C$. The sensitivity is about 7.5 $mV/cal\ cm^{-2}\ min^{-1}$; and the deviation from a true cosine response is within ± 2% for incident angles of 0° to 80°. An important, improvement over the older device is the provision of an optically ground Schott WG 7 glass envelope in place of the blown glass bulb used in 180° pyranometer. See figure 2.16.

The instrument is rated second class by the World Meteorological Organisation (WMO).

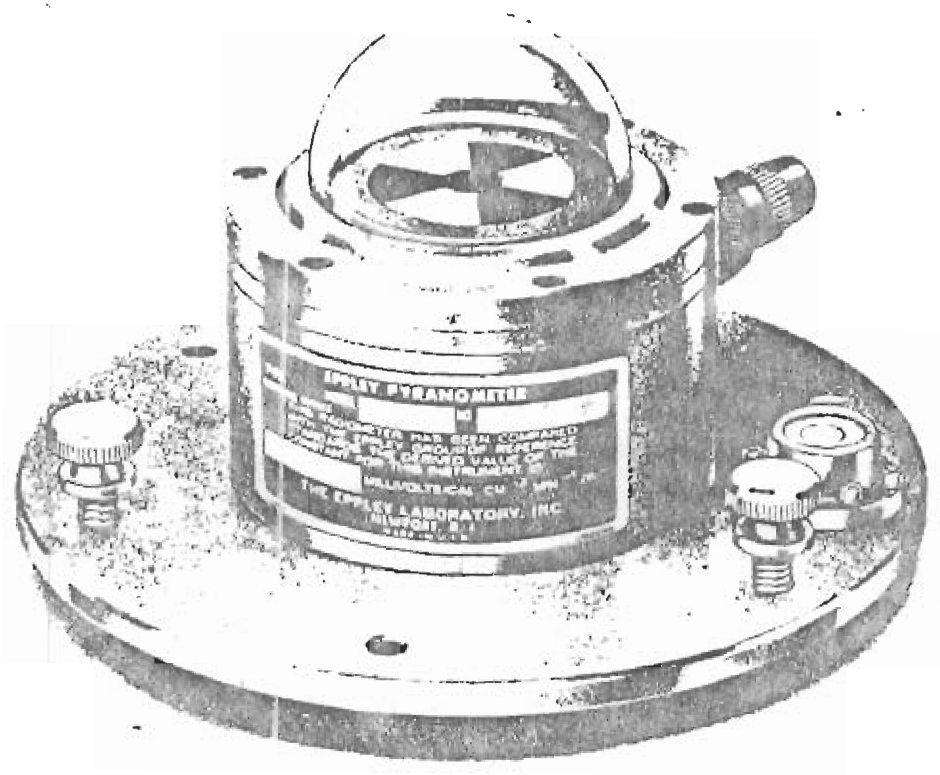

Fig. 2.16 The Eppley "black-and-white" pyranometer (courtesy of the Eppley Laboratories).

2.5.3 EPPLEY PRECISION SPECTRAL PYRANOMETER

The principal improvements on this instrument over the earlier types are

(a) Electrical compensation for the dependence of sensitivity on ambient temperature.

(b) Optical compensation for deviation of response from the Cosine law,

and

(c) Provision for the use of broad band spectral filters.

The detector for the original model was a conventional type of bismuth-silver thermopile of 15 junctions yielding about 7mV/cal CM^{-2} min^{-1}. A second version of the precision instrument, which is the model in current production, is considerably smaller in size than the original version and utilises a thermopile of copper electro plated on constantan wire over one half of each turn of a wire wound thermopile. See fig. 2.17.

The sensitivity of the instrument is 5mV/cal CM^{-2} min^{-1} approximately, with an impedence of 300 Ohms. The temperature dependence is $\pm 0.5\%$ from -20° to $40^{\circ}C$ and the Cosine error is $\pm 1\%$ over angles of 0° to 80°. Its response time (i/e) is 1 sec. with a linear response up to 4 cal CM^{-2} min^{-1}.

The instrument has two glass hemispheres, the outer of which can be replaced, with Schott colour filters for measurements of solar radiation in selected spectral bands. The use of spectral filters causes an apparent change of sensitivity. This is as a result of an increase of temperature of the filter glass by the absorption of solar radiation, with a consequent heating of the inner - glass hemisphere and modified long-wave radiative distribution of the detector.

The instrument is rated first class by the World Meteorological Organisation (WMO).

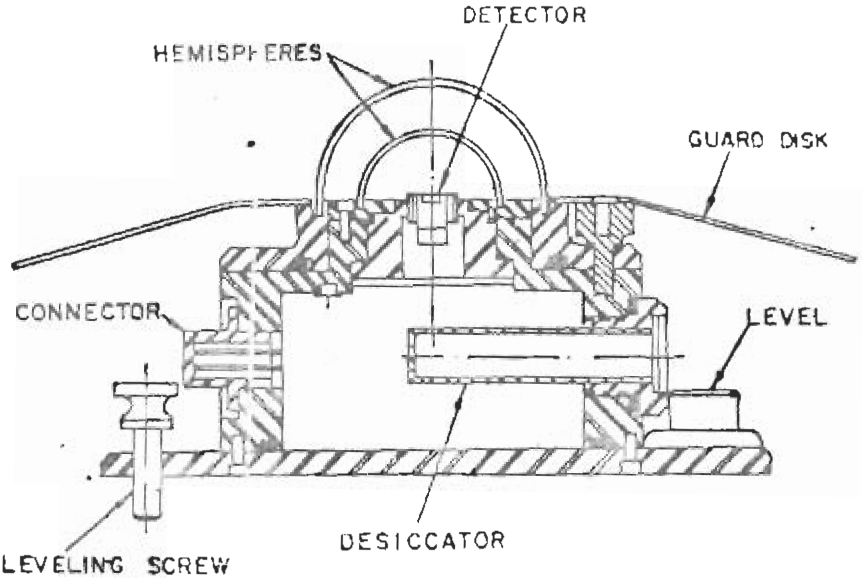

Fig. 2.17 Cross-sectional diagram of the current model of the Eppley precision spectral pyranometer (courtesy of the Eppley Laboratories).

2.5.4 MOLL - GORCZYNSKI PYRANOMETER SOLARIMETER

This instrument is based on the thermopile designed by DR. W.J. Moll (1923)[21]. The thermopile consisted of no less than 80 thermocouples arranged inside a circle of about 2 cm diameter, and gave up to 16mV for incident radiation of 1g cal cm^{-2} min^{-1}. The rapid response of the thermopile to changes of incident radiation, the very small dependence on ambient temperature, and the essentially linear relationship between radiation intensity and instrument response all boded well for the future of the Moll thermopile in radiation measurement

The basic design of the Moll thermopile is shown in fig. 2.18. The thermojunctions are made of very thin (0.005mm) blackened strips of manganin and constantan which are joined at point B and soldered at points A and C to copper posts are clamped to a thick brass plate G. A thin coat of lacquer between the posts and plates provides electrical insulation without sacrificing good thermal contact. The active junctions are normally arranged along a line through the centre of the plate, and the passive junctions are on top of the copper posts. The small heat capacity of the strips and efficient heat conduction to the copper posts assures a small lag coefficient and the large heat capacity of the brass plate with copper posts assures approximately constant temperature and makes it unnecessary to shield the passive junctions from the incident radiation.

The thermopile of the current model of the Moll - Govczynski pyranometer consists of 14 blackened Manganin - constantan thermoelements arranged in a 12 X 11 mm rectangular configuration. It is protected from the atmosphere by two concentric hemispherical glass-domes - see fig. 2.18b, which can be removed for inspection and cleaning. Condensation of moisture on the inside of the dome is prevented by the enclosed spaces being filled with a desiccant, such as silica gel. The 30-cm diameter radiation shield surrounding the outer dome, and co-planer with the sensitive element, prevents direct solar radiation from heating the base of the instrument. The domes have uniformly high transmission characteristics throughout the spectral range of

$$\lambda = 0.32\mu m \text{ to about } \lambda = 2.5\mu m.$$

The transmission falls off steeply beyond $2.5\mu m$. Sensitivity of the instrument is 8 - 9 mV/cal cm^{-2} min^{-1}, and the internal resistance of the thermopile is approximately 10 Ohms. The temperature coefficient amounts to $0.00015 - 0.0020\,^{\circ}C^{-1}$ in the sense of decreasing sensitivity with increasing temperature. No temperature compensation is provided in the instrument.

Deviation from cosine law is within 1% for incidence angles of less than 75%, with greater and individually variable deviations at larger angles of incidence. These deviations from the exact Cosine response with angle of incidence of the radiation, and changes of response with azimuth of the incident radiation result are mainly from imperfect reflection or absorption characteristics of the coatings on the selective elements.

The instrument is rated second class by the World Meteorological Organisation (WMO).

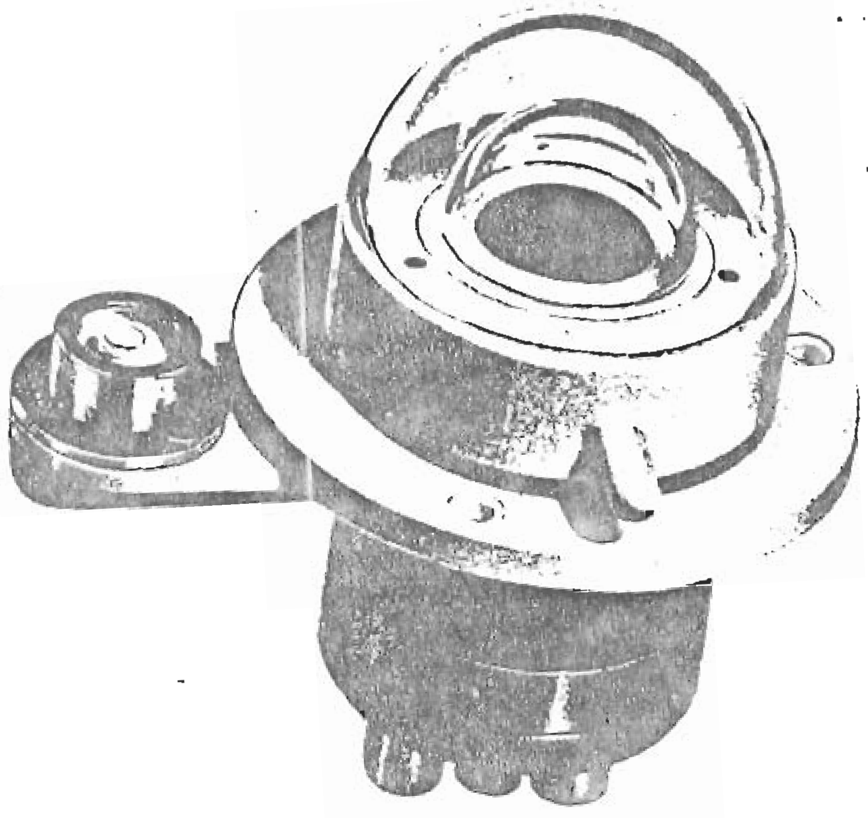

Fig. 2.18 The Moll-Gorczynski pyranometer as manufactured by Kipp and Zonen (courtesy of Kipp and Zonen).

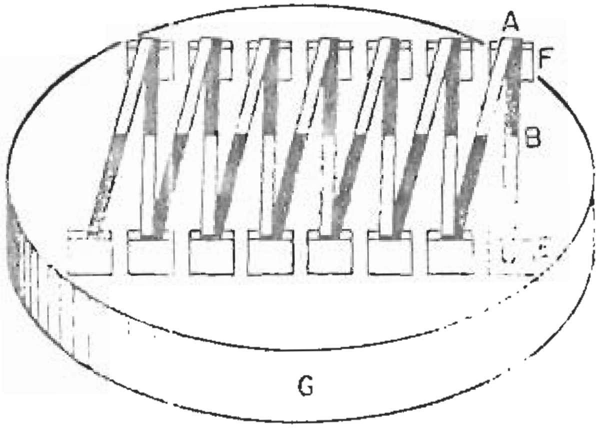

Fig. 2.18b Diagram of the Moll thermopile. B, active junctions of metal strips; A and C, passive junctions of metal strips; E and F, copper mounting posts; G, massive brass plate.

2.5.5 YANISHEVSKY PYRANOMETER

This pyranometer is the principal instrument for measuring diffuse solar radiation, global solar radiation, and surface albedo in the USSR. The sensor is constructed either in a square checker board pattern of alternate black and white squares and rectangles or in a radial pattern of alternate black and white segments as shown in fig. 2.19. The thermo couples are composed of alternate strips of manganim and constantan. The hot junctions are blackened with soot and the cold junctions are whitened with magnesium. The sensor assembly is covered with a single glass hemisphere, and an auxilliary opaque hemisphere is provided for obtaining the zero setting. Condensation of moisture inside the glass is prevented by the use of a drying agent in a cavity set into the base of the instrument.

Older models of the instrument suffered a defficiency due to the thickness of the paint on the sensing elements. The metal strips were very thin but the layer of paint was thick enough to cause a significant roughness to the surface. This roughness in combination with space between the elements, caused a deviation from the Cosine law. In the newer models there are no significant spaces between the elements, and the paint is of uniform thickness over the whole sensing surface. The construction is of three rings; two of manganin and one of constantan, set close together and cut into narrow radial strips. These strips are then painted black and white as shown so that an approximately

plane surface is obtained. The instrument is used in either of two models of operation for measuring surface albedo. The usual method is to employ two instruments, one facing upward and the other down ward, the albedo being simply the ratio of the resulting two measurements. This pyranometer is used as a relative instrument, and therefore requires calibration against a standard. The operational method of calibration is against a standard. The operational method of calibration is by the sun - shadow method, with the Angstrom Pyrheliometer as the primary standard.
It is rated second class by the World Meteorological Organisation (WMO).

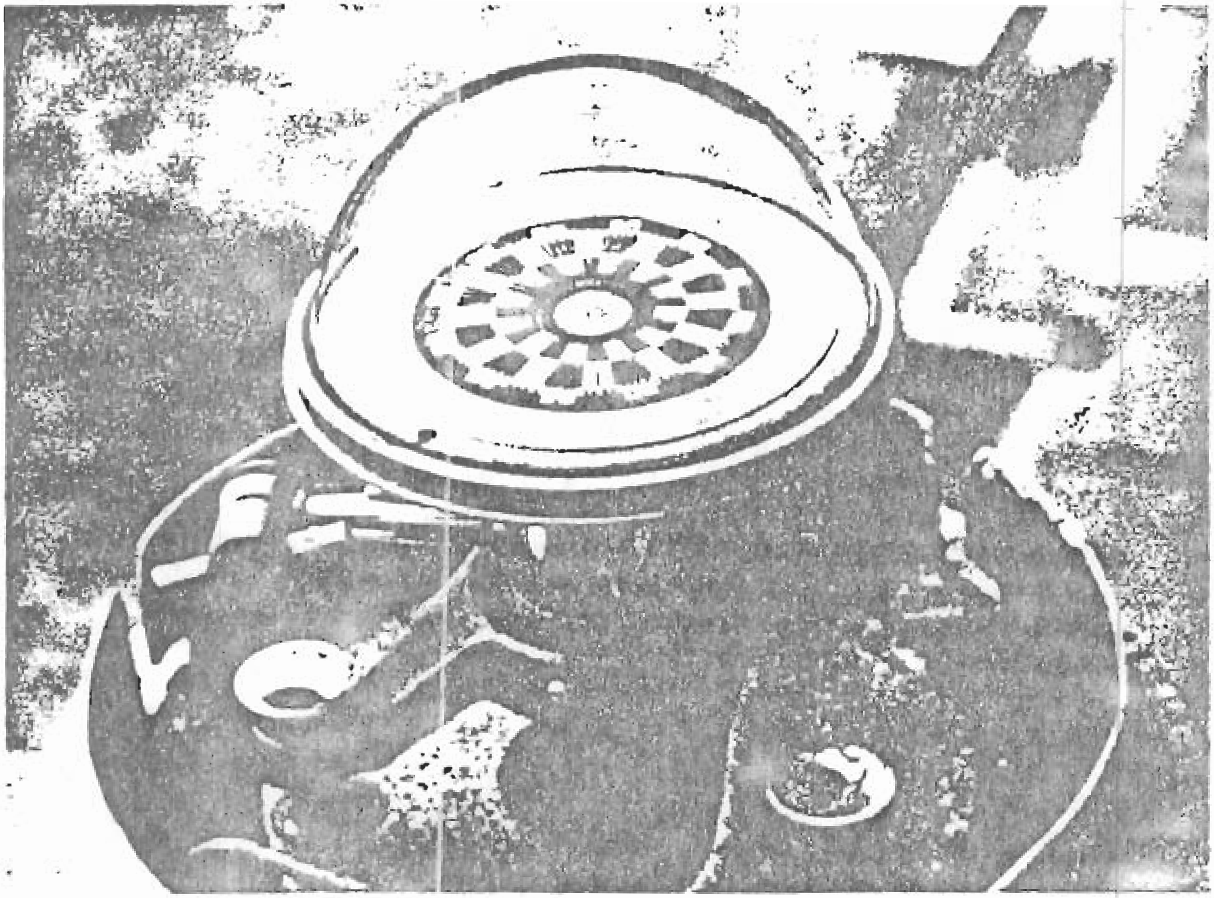

Fig. 2.19 Photograph of the Yanishevsky pyranometer in operation at the Radiation Observatory, University of Moscow (photograph by author).

2.5.6 ROBITZSCH BIMETALLIC PYRANOMETER - ACTINOGRAPH

A number of models of the Robitzsch - type instruments are available, but all are basically similar to that shown in fig. 2.20. The main sensor is a blackened bimetallic strip of dimensions about 8.5 cm X 1.5 cm which acts simply as a bimetal thermometer. One end is free to move as changes of temperature causes a distortion of the strip. Through a mechanical linkage the movement of the free end of the blackened strip causes a deflection of a recorder pen which makes a trace on a recorder chart mounted on a clock-driven drum. Two standard speeds of rotation of the drum are available; one full rotation in 24 hours and the other, one full rotation in 7 days. For operation the entire mechanism is enclosed in a sealed, desiccated metal case, the main sensor section being covered by a hemispherical glass dome. A window is provided for viewing the pen and recorder chart.
See figure 2.20.

Since the amplitude of the deflection of the bimetallic strip is determined entirely by its temperature, the instrument is sensitive to the ambient environment as well as to the flux of incident radiations. Changes in the calibration have been found to be very large for this type of instrument. Because of its distortion with temperature the blackened sensor strip cannot remain flat, a fact which makes the calibration. Constant a function of both azimuth and zenith angle of the incident radiation. Additional effects such as imperfections in the glass of the dome and non uniform concentration of energy by caustics produced by the glass contribute to the directional sensitivity of the calibration factor. The large heat capacity of the bimetallic temperature element and its associated mountings result in a slow response of the instrument to changes of incident flux energy. The time constant varies between the different designs. 10 - 15 minuses are normally required for a 98% response to a sudden change of energy.

Spectral transmission of the glass dome is apparently not uniform among various models available, but it is normally greater than 90% over the range 0.4 m to 2.0 m.

In summary, with the best design which has been developed so far, the Robitzsch - type instruments are suitable only for daily total radiation measurement in which accuracy of ± 10% is adequate. It is rated third class.

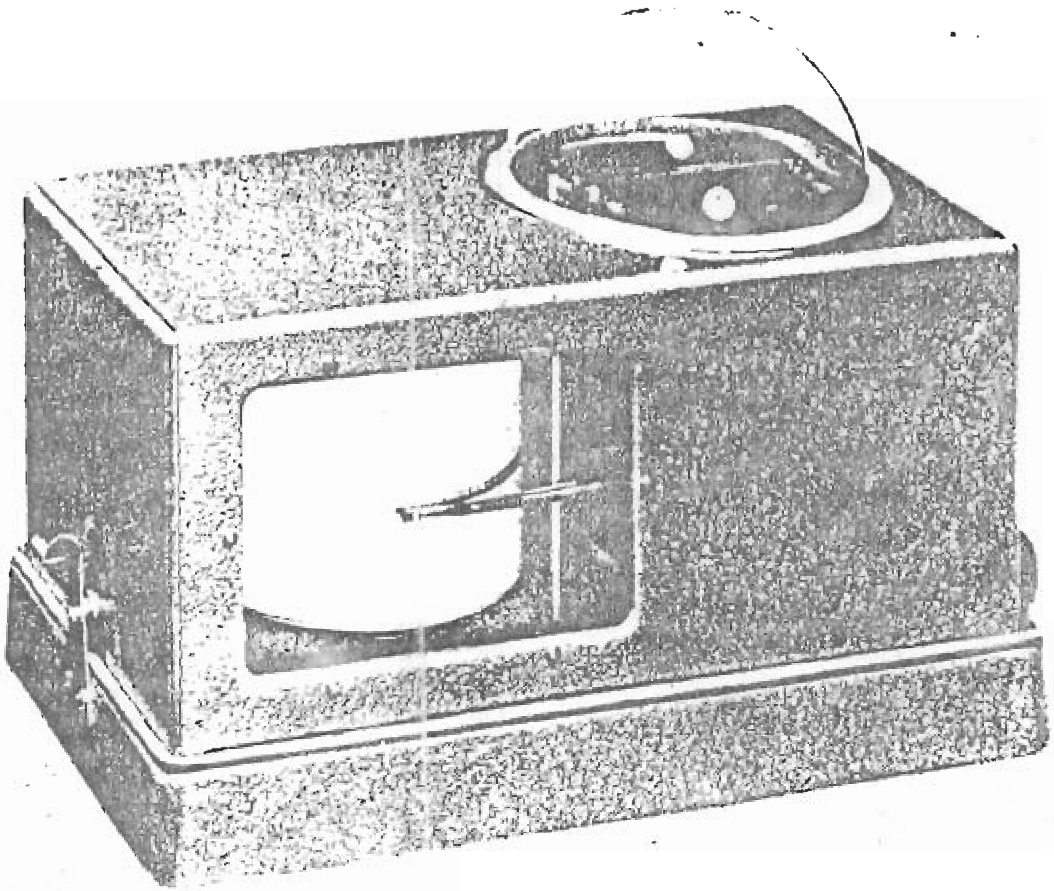

Fig. 2.20 The Robitzsch bimetallic pyranometer (actinograph) (courtesy of Science Associates).

2.5.7 DIRMHIRN AND SAUBERER (STAR) PYRANOMETER

This instrument utilizes 32 (16 in some models) copper plates, half of which are covered with a highly reflective white paint, and the other half are blackened for high absorptivity. The two sets of plates are mounted as alternate black, and white segments radiating as a 'Star' from a central point, together forming a flat circular disk - see fig 2.21.

The two types of plates are thermally isolated from each other by being mounted on poorly conducting concentric rings which are themselves thermally isolated from the main base plate of the instrument. Thermo-junctions of either copper - constantan or manganin - constantan are soldered to the under side of the copper plates, hot junctions being attached to the black segments and cold junctions to the white segments.

The sensor disk is covered by a ground and polished glass hemisphere which transmits more than 90% of the solar radiation through the 0.3 to 3.0 um spectral range. The sensor sector is hermetically sealed and the enclosed air is in contact with a drying agent which eliminates moisture condensation on the inside of the glass hemisphere. The sensor assembly is enclosed in a circular housing painted white to minimize radiant heating effects. The circular symmetry of the receiving disk eliminates any azimuth dependence of sensitivity, and measurements available indicate a relatively true cosine response down to an incidence angle of 75°. The instrument response is closely proportional to radiant intensity. Temperature compensation is not included, but the

temperature coefficient is sufficiently low as to make temperatu
compensation unnecessary for most observational condition.
See figure 2.21.

The pyranometer has found relatively wide acceptance in various parts of the world, and is rated second class by the World Meteorological Organisation (WMO).

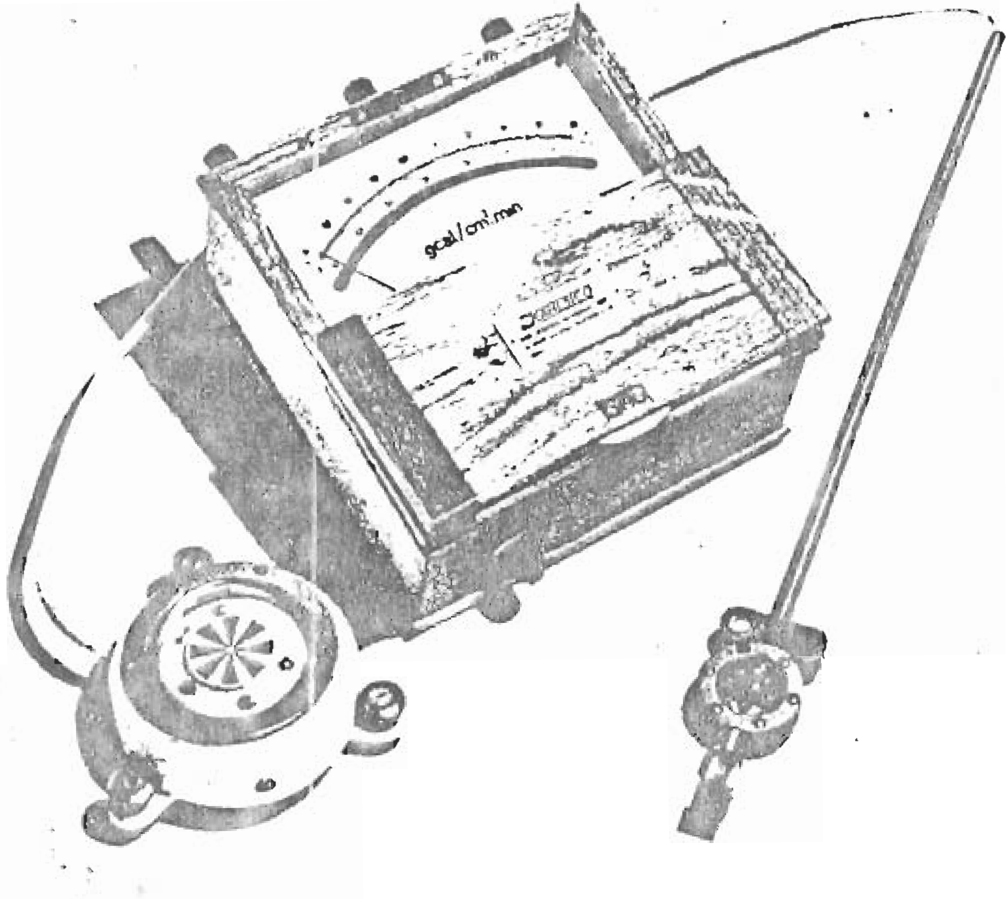

Fig. 2.21 The star pyranometer (lower left) with a directly indicating meter and a radiation balance probe (courtesy of the Kahl Scientific Instrument Corp).

2.6 CALIBRATION OF PYRANOMETERS

Unlike pyrheliometers, there are no absolute pyranometers. All pyranometers are calibrated instruments. There are a number of methods of calibrating pyranometers using the sun or laboratory sources. Two methods commonly used are calibrating directly against a reference standard pyrheliometer using the sun as source and calibrating against a reference pyranometer that has already been calibrated.

2.6.1 CALIBRATION AGAINST A REFERENCE STANDARD PYRHELIOMETER

Calibration of the reference pyranometer is accomplished by transfer of calibration from an absolute pyrheliometer by means of a shading method. A perfectly clear day should be chosen to conduct this calibration.

In the shading method, simultaneous measurements are made with the pyranometer and the absolute pyrheliometer. At regular intervals, a disk is interposed between the sun and the pyranometer. The disk should be large enough to shade the glass dome at all zenith angles. For example, a disk 10 cm in diameter and held 1m from the pyranometer will approximate a six degree aperture angle of the reference standard pyrheliometer A value of the vertical component of the direct radiation is obtained from the difference of separate measurements of the global (direct plus diffuse) and diffuse irradiance.

The pyranometer calibration factor, K is obtained from the pyranometer value of the vertical component (in voltage units) divided by the irradiance value of the vertical component obtained from the absolute pyrheliometer (i.e measured direct component times the sine of the solar elevation angle).

Thus

$$K = \frac{\text{Pyranometer reading averaged over the exposed period minus that averaged over the shaded period}}{\dot{I}_n \cos \theta_s}$$

where $\dot{I}_n$ is the direct normal irradiance calculated from the pyrheliometer reading.

Shade calibration is also performed over a wide range of solar elevation of sensitivity with solar angle (i.e the cosine response). During the shade calibration, a second pyranometer should be operated, but not shaded to measure continuously the global irradiance. Ratios of the voltage outputs from the two pyranometers during non-shading periods are then used to obtain an estimate of what the non shaded voltage would have been for the test instrument at the time it was shaded. At the same time the occulting disk should alternately shade and expose the pyranometer for duration of about 10 minutes.

Shade calibrations are recommended only for reference pyranometers. It is not recommended to make shade calibration of instruments whose sensitivity varies with the wavelength of the irradiance.

2.6.2 CALIBRATION AGAINST A REFERENCE PYRANOMETER

This is the calibration technique now preferred to other calibration methods. It is based on out door comparisons. In this procedure, the reference pyranometer and the test pyranometer are operated side by side for periods of about two weeks. Daily calibration values for the test pyranometer are obtained using the complete day light period, the final calibration value is the average of the daily values. Days with prolonged periods of rain, snow or low over cast cloudiness are not included in the final average. The final average does, however, represent a variety of clear and cloud conditions. The reference pyranometer is an all - black first class thermopile pyranometer while several other pyranometers are included in all calibrations and serve as controls to detect changes in the reference pyranometer. The calibration factor is the a ratio of the measurement from the test pyranometer to the measurement from the reference pyranometer.

The major advangage of the out door calibration method is that all types of pyranometers are referenced to a single reference (whose calibration has been directly obtained from an absolute pyrheliometer) under realistic irradiance condit

The main disadvantage is that the natural environment is not subject to control and therefore the calibrations include all the instrumental characteristics of both the reference and test instrument which are influenced by the

2.7 PYRANOMETER CHARACTERISTICS

In designing pyrheliometers and pyranometers, there are a number of common considerations for attaining high accuracy in measurement. These considerations include for example: sensitivity, stability of calibration factor, linearity, change in response due to variations in ambient temperature, spectral response of sensor, response time, and effects of auxilliary equipment. The effect of circumsolar radiation, which depends on the aperture angle, is a unique factor in the case of pyrheliometers. On the other hand, the directional response of the sensor on the elevation and azimuth of the sun and the effect of inclination of a pyranometer are problems specific to the instrument.

2.7.1 COSINE EFFECT

The sensing element of pyranometers is invariably coated with a highly absorbent black paint. Although it is easier to achieve high absorptance in the spectral sense, it is difficult to achieve the same in the directional sense. That is, absorptance varies with the angle of incidence. Most surfaces exhibit an angular dependence of absorptance. This variation is not identical for electrical non conductors and electrical conductors. For most electrical conductors, absorptance remains almost constant until the incident angle exceeds about 70°. Beyond this point, absorptance increases considerably and then drops rapidly when the angle of incidence approaches 90°. Fig 2.2 shows this characteristic qualitativel[y]. This angular dependence of absorptance is called the cosine effect. Fortunately, at low solar elevation the energy contained in the solar beam is very small. In a well-designed pyranometer this variation should not exceed 2%.

Many authors have investigated tilt effects on pyranometers. However, because of continuous developments and modifications in pyranometry Manufacturers catalogues should be consulted in order to carry out any corrections necessary. For example, the Eppley laboratory recommends no tilt correction for its "black and white" and also for precision spectral pyranometers. Kipp and Zonen[22] provided a correction plot for one of their pyranometers.

2.7.2 AZIMUTH EFFECT

Under ideal conditions the response of a receiver is proportional to the cosine of the angle of incidence and is constant at all azimuth angles. However, real surfaces contain some imperfections arising from the manufacturing processes and consequently small variations in azimuthal absorptance do occur.

2.7.3 EFFECT OF INCLINATION

In many solar energy applications it is necessary to measure insolation on inclined planes. A pyranometer mounted on an inclined plane receives from a solid angle of 2π direct, sky diffused, and ground reflected radiation. Since pyranometers and calibrated in a horizontal upward direction, they may show a change in response when mounted in an inclined or downward direction. This change occurs mainly because of a hemispherical glass dome. This tilt effect varies with the angle of irradiance. For some models, such as Kipp and Zonen pyranometers, it also varies with the orientation of the thermopile vis-a-vis tilt angle. Deviation from the horizontal position increases with the tilt angle and with the level of radiant flux. In a well - designed pyranometer this variation should not exceed 2%.

Many authors have investigated tilt effects on pyranometers. However, because of continuous developments and modifications in pyranometry, manufacturers' catalogues should be consulted in order to carry out any corrections necessary. For example, the Eppley laboratory recommends no tilt correction for its "black and white" and also for precision spectral pyranometers.

Kipp and Zonen[23] provide a correction plot for one of their pyranometers.

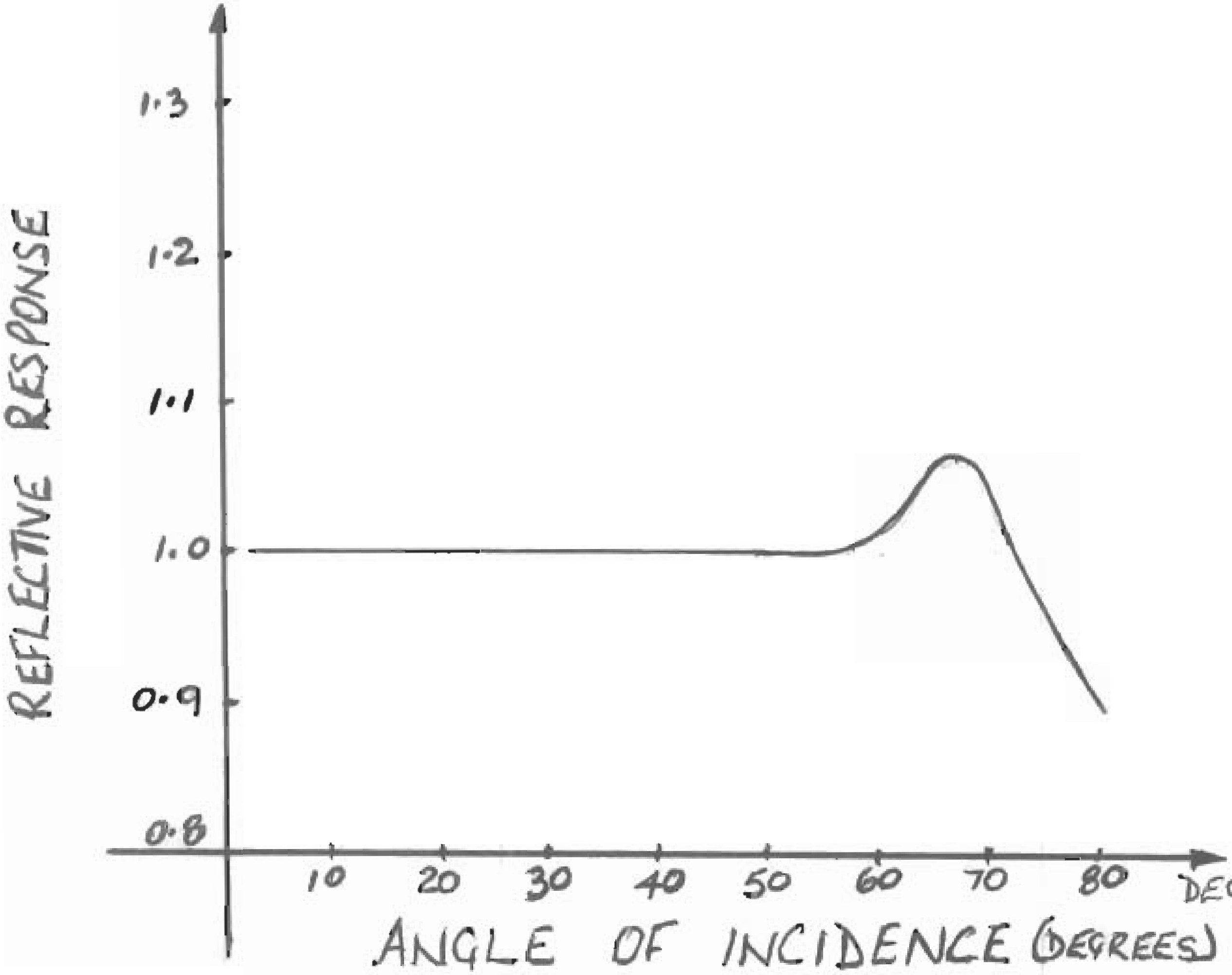

Fig. 2.22 pyranometer response as a function of the angle of incidence.

2.8 INSTALLATION OF PYRANOMETERS

The process of installation of pyranometers varies with types of instruments. However, some general principles apply to all pyranometers.

The essential requirement in installation of a pyranometer is that of proper exposure. Basically, the sensing element for the hemispheric type pyranometer should be above

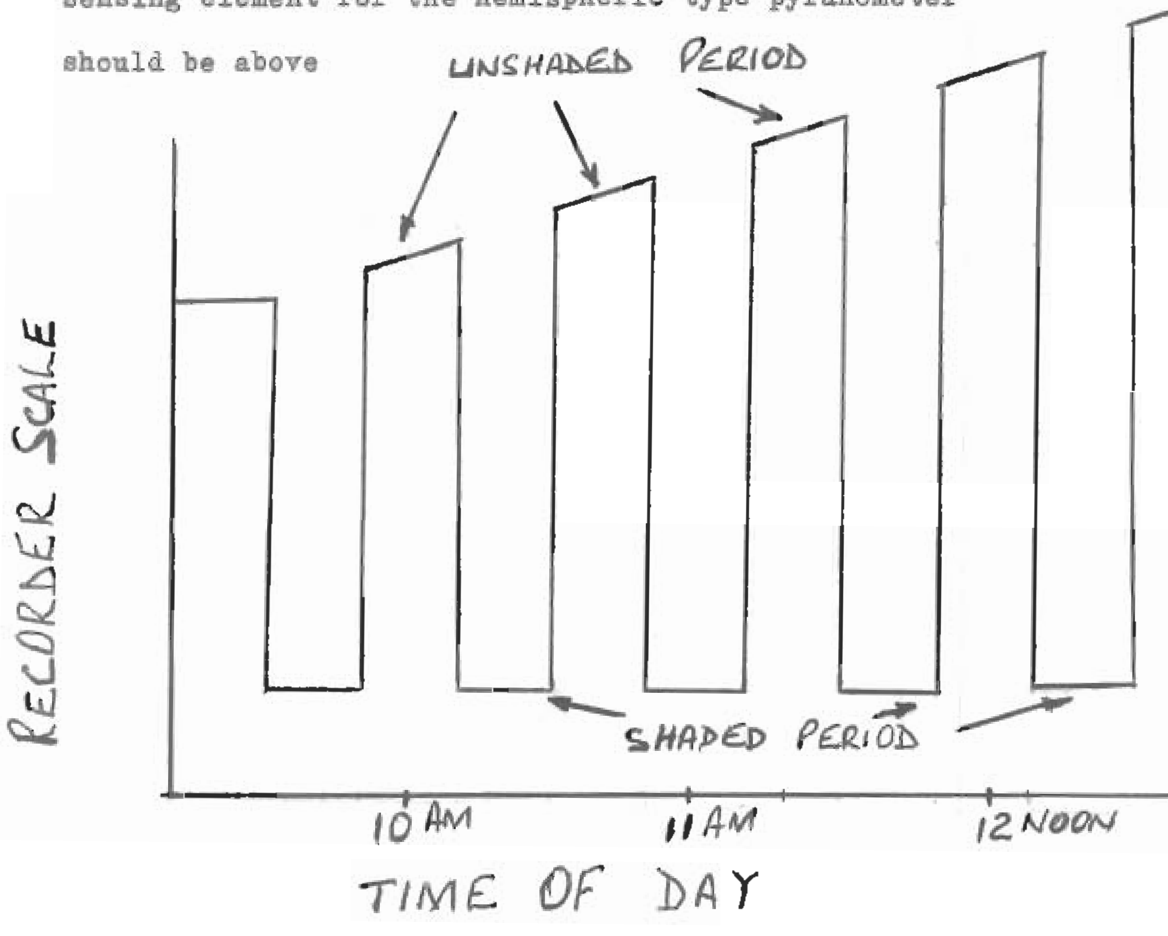

Fig. 2.23 pyranometer response with and without a shading disk.

all surrounding obstacles such as buildings, trees, hills, mountains, etc. so that the radiation reaches the instrument from the entire hemisphere of the sky. In practice, however, it is normally difficult to realise such an ideal situation. Therefore compromises are sometimes made when making measurements. Obstacles which cut off direct solar radiation from the instrument, cause the most errors. Thus, it is necessary to avoid in particular, such obstructions in the easterly or westerly directions.

A transit or theoddite could be used to map on a diagram of azimuth versus elevation angles, the outline of an obstacle and hence determine the solid angle which it substends at an instrument. While some obstacles reflect solar radiations, others such as black body obstacles, diminish the diffuse flux on a unit horizontal surface. Because of these problems, it is preferable to choose a location for the pyranometer such that the error in measurement due to an obstruction is less than that introduced by other factors.

The pyranometer should also be easily accessible for practical purposes. For instance, the glass envelope has to be kept free of dust or other deposits by frequent cleaning and shadow rings or disks, when used, should be adjusted regularly (say every 2 or 3 days) for change of declination of the sun.

CHAPTER THREE

3.0 EXPERIMENTAL DETAILS

3.1 DESIGN AND CONSTRUCTION OF THE PYRANOMETER USING AVAILABLE LOCAL MATERIALS

The design of the pyranometer is similar to that of Eze (1983) and that of Asogwa (1990)[24]. However, some modifications were made in their designs in order to improve on their work. The major modification in our design when compared to Eze's is that the operational amplifier is dispensed with. The output from the pyranometer is fed into a sensitive long scale galvanometer. The advantage of this system is that the readings are not seriously affected by small changes in power supply. Also the thermopile was calibrated before assembling to give more accurate readings. The main difference between this design and Asogwa's are that the base of the box is seasoned solid plywood. The advantage of this is that solid plywood is more durable since ordinarily plywood wears-off with time depending on weather condition.

Also a white perspex glass of greater thickness (5mm) is used. This has the advantage of giving greater protective resistance to the casing against bad weather. Moreover, the aluminium foil was coated with white paint and it was covered with white chalk particles and finally sealed with another aluminium foil. This has the advantage of making the reflector surface highly reflective.

The absorber position is made adjustable so that one can easily vary the distance between the absorber and the reflector. This may have the advantage of increasing the value of the E.M.F.

The pyranometer was constructed in parts and then assembled. The essential features of the pyranometer are:

(A) THE THERMOPILE

The termopile consists of four copper - constantan thermocouples measuring 100cm. A prototype of the thermocouple is shown in fig. 3.1 below.

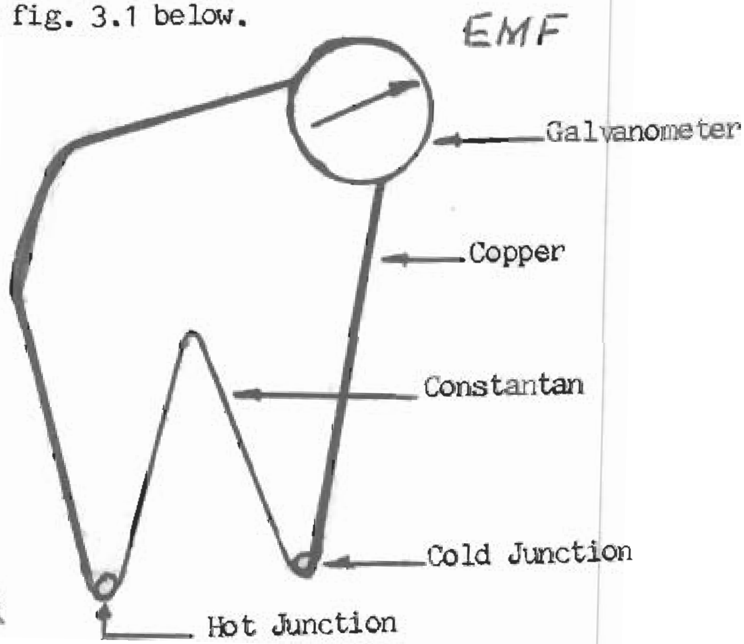

Fig. 3.1 THE THERMOCOUPLE

The thermocouple was constructed by cutting out 100cm lengths of copper and constantan wire and then soldering them together as shown in fig. 3.1. The e.m.f developed by a single thermocouple is very low. In order to increase the e.m.f developed, a number of thermocouple junctions were connected as shown in fig. 3.2.

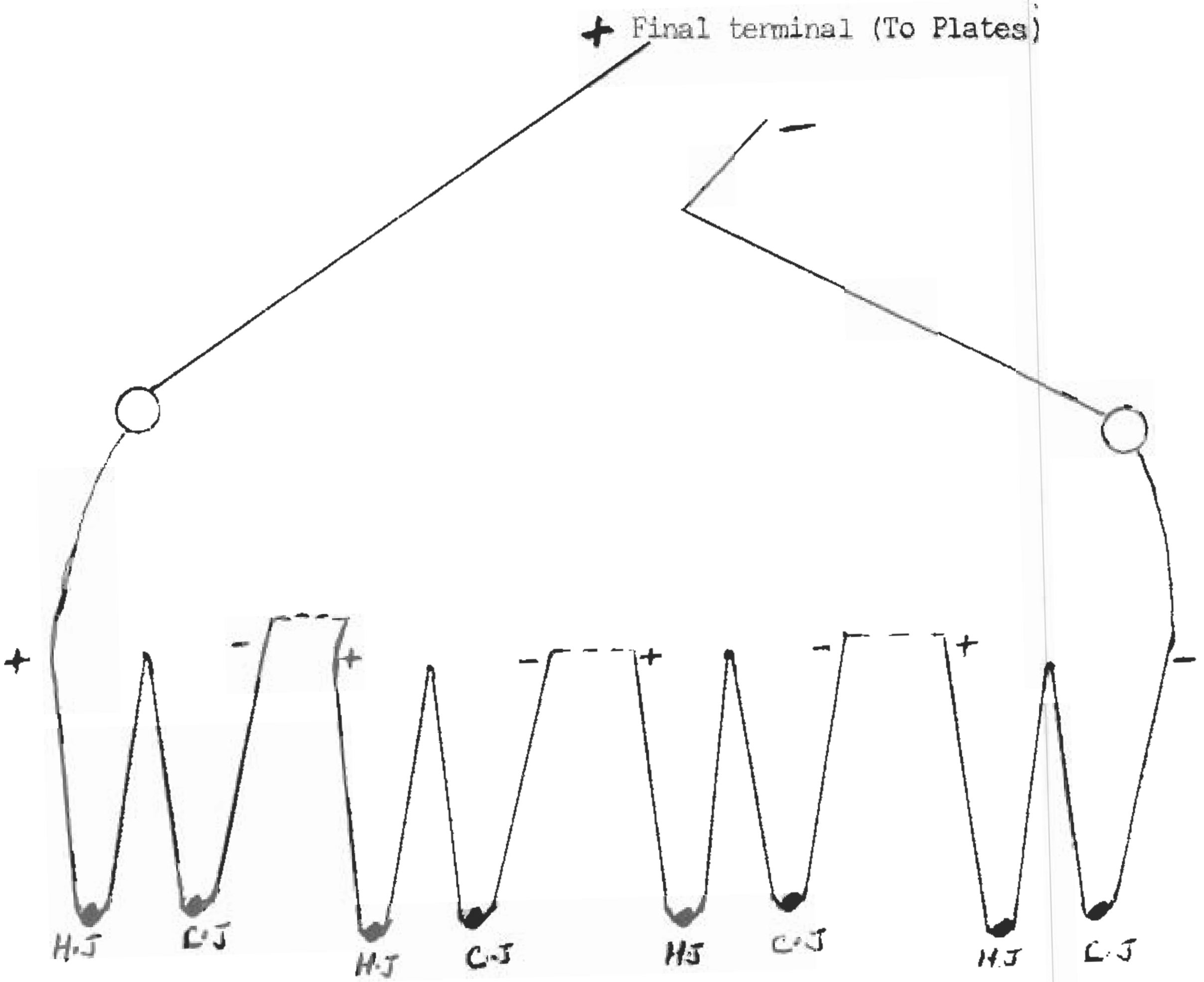

Fig. 3.2 (THERMOCOUPLE JUNCTION IN SERIES)
(THERMOPILE)

Theoretically E.M.F developed by a thermopile is given by

$$E.M.F = \alpha (T_1 - T_2) + \beta (T_1 - T_2)$$

where α and β are constants

$$\alpha = 40\ \mu V/^{\circ}C = 0.04 MV/^{\circ}C.$$

β is very small. Therefore, $\beta (T_1 - T_2)$ can be neglected.

Therefore, $EM.F = 0.04(T_1 - T_2)$

where T_1 is the termperature of the hot junction and T_2 the temperature of the cold junction.

By connecting the junctions of the thermocouple in series, the e.m.f can be greatly increased.

(B) PROTECTIVE BOX (INSTRUMENT CASING)

The mounted thermopile is housed in a box of 24cm x 24cm x 8cm built out of an acrylic plastic material (perspex). The edges of the box are joined chemically with plastic binding cement. Bending of the strip of perspex measuring 100cm x 8cm was done on a locally built plastic bender, belonging to the department of Mechanical Engineering, University of Nigeria, Nsukka. (Courtesy of Mr. E.U. Ekpo).

The top of the box is covered with white perspex to reflect all radiations falling on it. The base of the box on which the T - shaped stand carrying the thermopile is mounted is made of wood and is detachable by undoing four screws. A hole 15cm in diameter is cut in the centre of the perspex top. This was made by drilling a small hole and then filing to size. The top is fixed to the dome by means of an adhesive. The wooden base which carries the thermopile forms the base of the box. The protective box is shown in fig. 3.3.

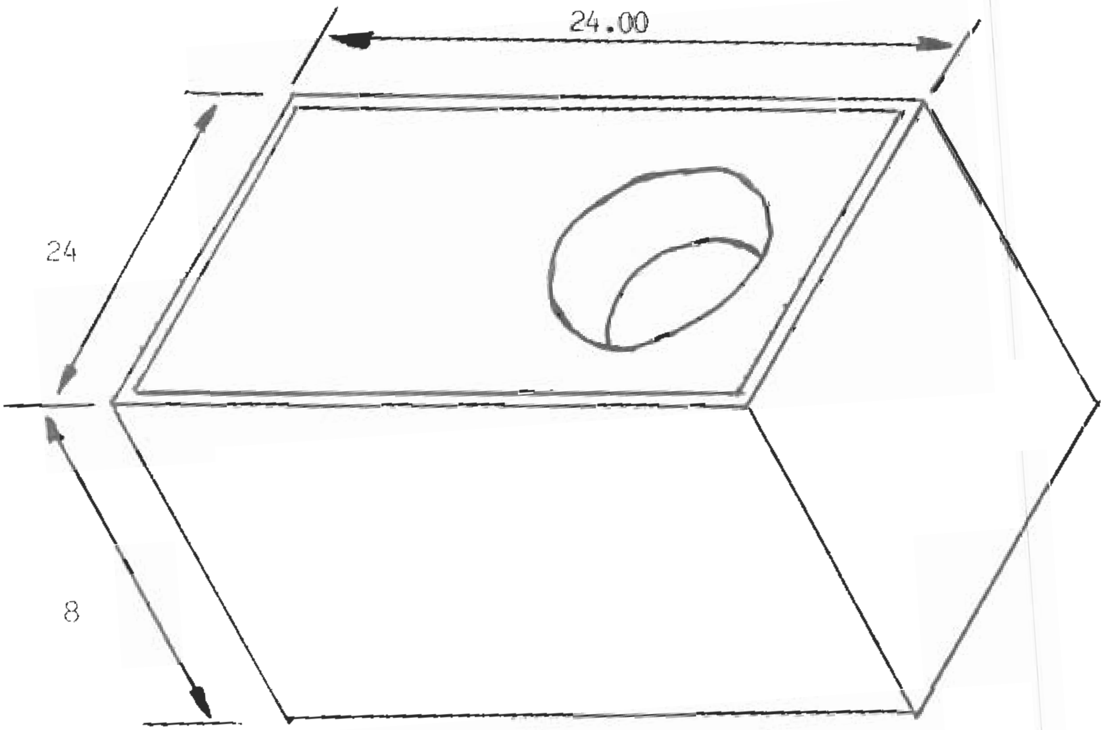

Fig. 3.3 FINISHED PRODUCT OF CONSTRUCTED PYRANOMETER CASE (DIMENSIONS IN CM)

Fig. 3.4 The Thermopile shown in its position

(D) <u>RADIATION SENSOR</u>

The radiation sensor consists of a set of five copper plates (one large one and four smaller ones) to which four copper - constantan thermocouples are connected.

Each of the four smaller copper plates measures 3cm x 2cm x 1cm while the larger one measures 8cm x 4cm x 1cm.

The plates were first thoroughly cleaned with concentrated tetraoxo sulphate (IV) acid H_2SO_4 and then dried with emery-paper. Each/plates was perforated at the middle where one junction of one of the thermocouples was soldered to one of the small plates. The other set of four junctions was soldered to the large plate. Each of the four plates was blackened using a mixture of black paint and lamp black. The lampblack was added to give the surface a matt finish. This increases their absorbance. The thermocouple junctions connected to these black plates act as the hot junctions (positive terminal). The large plate was painted white and then covered completely with aluminium foil. This makes the surface highly reflective. The junctions connected to this plate are the 'cold' junctions (negative terminal).

The plates are then screwed into T-shaped insulating supports which are fixed to a wooden base as shown in fig. 3.5.

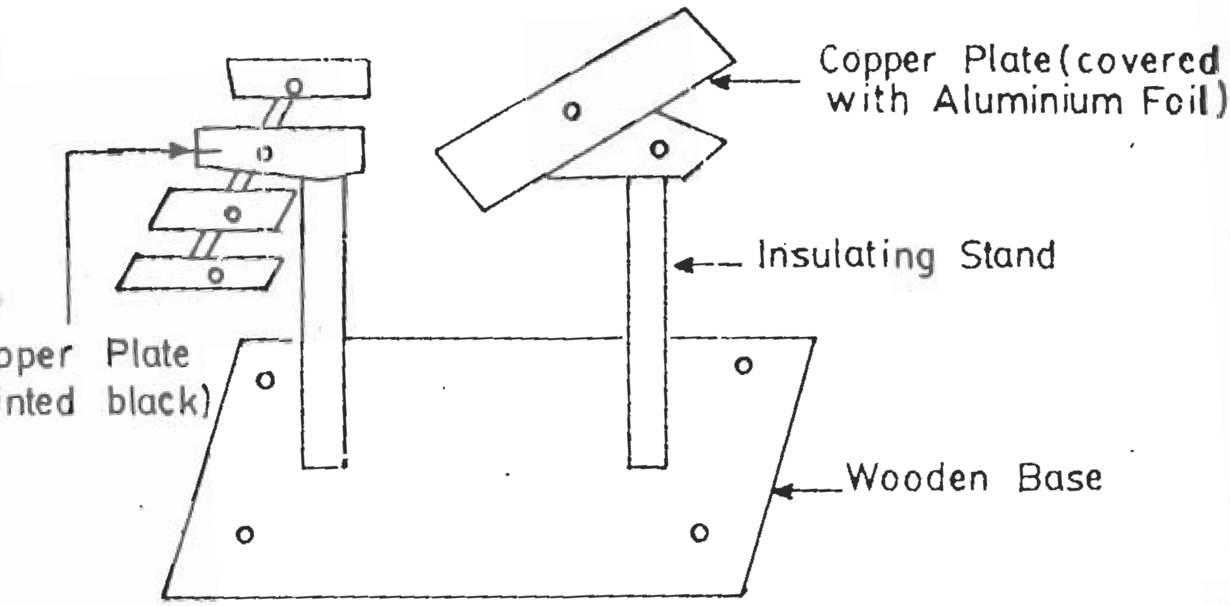

Fig 3.5 COPPER PLATES MOUNTED ON T-SHAPED INSULATING STANDS

(E) INSULATING STAND

This was construed out of two pieces of wood which were first cut to size with a saw and then shaped to a round shape on a lathe machine at the Department of Physics and Astronomy Workshop (Mechanical Section). The dimensions of the insulating stand are 10cm x 1.3cm. See fig 3.6

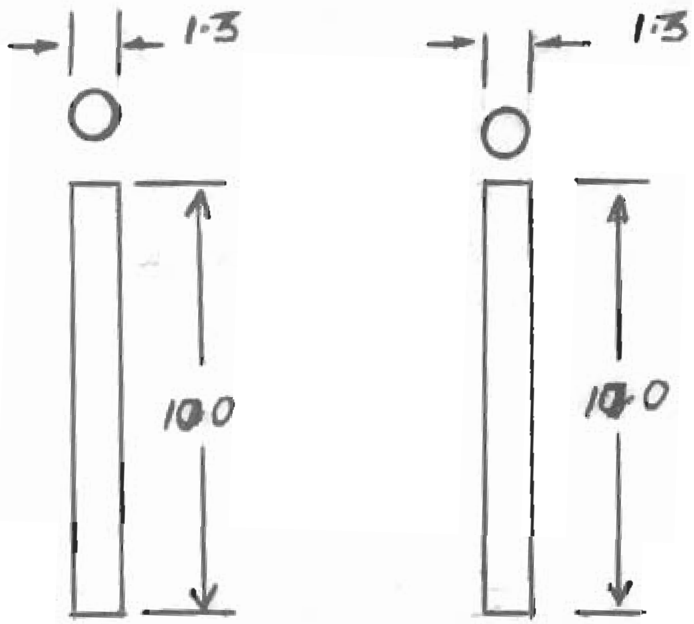

Fig. 3.6 INSULATING STANDS CONSTRUCTED WITH DIMENSIONS IN Cm

The pyranometer was now assembled as shown in fig. 3.7 after the construction of the different parts.

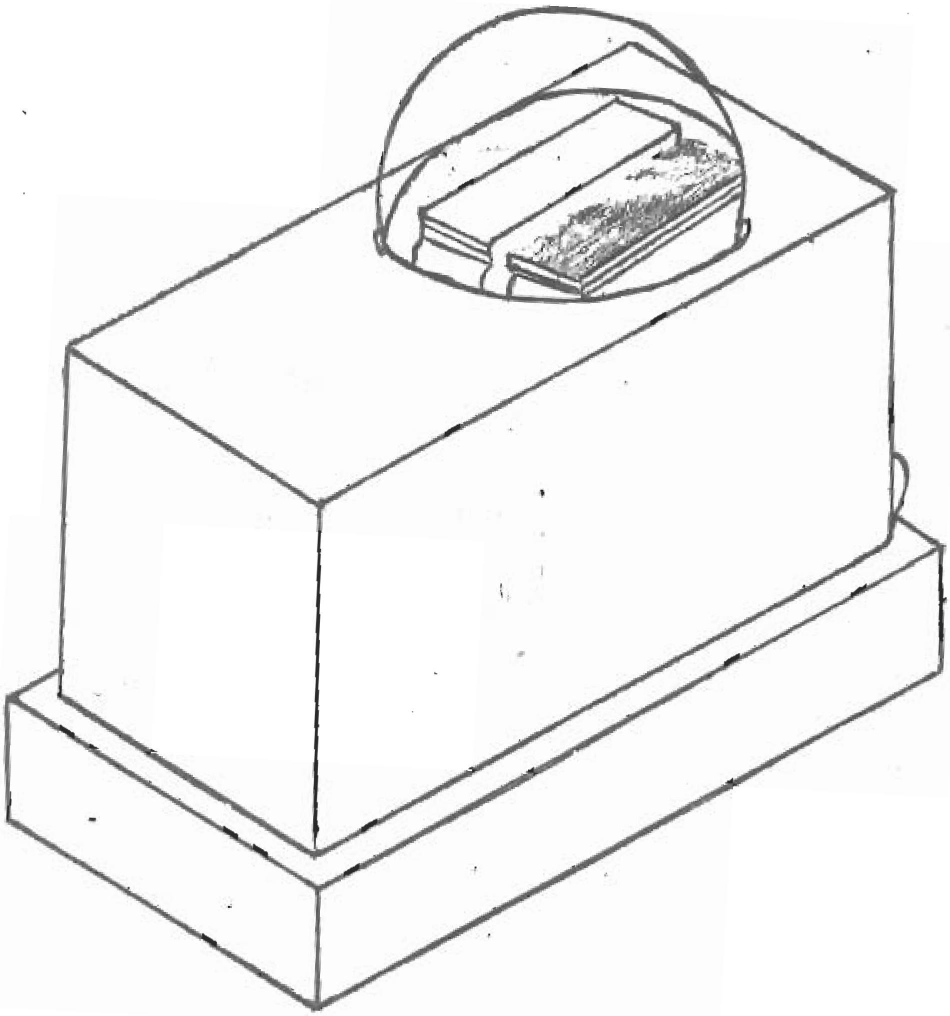

Fig. 3.7 - Constructed instrument in its operational mode.

The construction of the pyranometer now completed, the out put therm-electric e.m.f was checked. This was done by mounting the pyranometer outside where it received insolation. The thermo-electric e.m.f was measured when the insolation was almost at its peak that is, about 1.00 p.m. Many measurements taken showed that even at the peak insolation the e.m.f developed did not exceed 600U volts. It was therefore difficult to monitor small variations in the intensity of solar radiation. To overcome this problem, the pyranometer output voltage was monitored using an EDSPOT long range galvanometer (see fig. 3.8 and plate 1.

when the pyranometer was exposed to solar radiation and connected to the galvanometer, the deflection was observed to vary with the intensity of solar radiation.

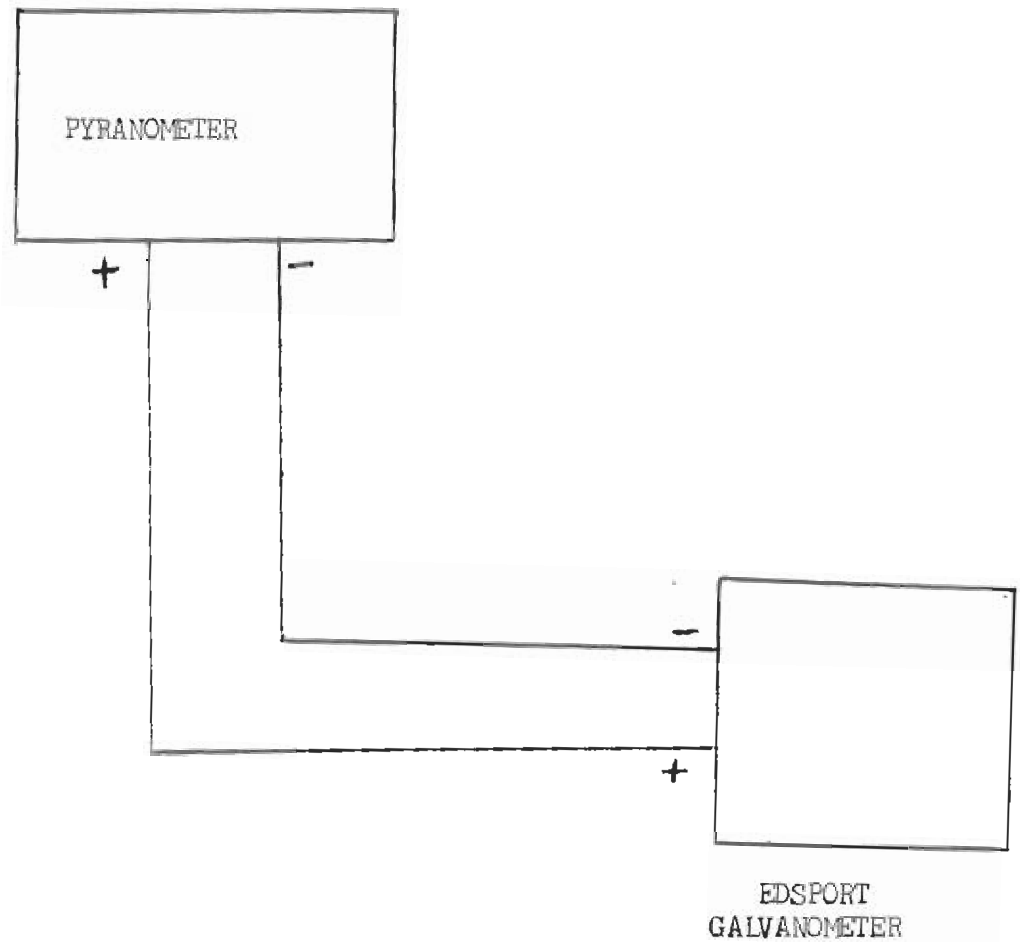

Fig. 3.8 CONNECTION OF CONSTRUCTED PYRANOMETER TO THE EDSPORT GALVANOMTER

3.2 CALIBRATION OF THE PYRANOMETER

The pyranometer was calibrated by taking readings at five minute intervals with the instrument for two days. During those days it was placed side by side with an Eppley integrator pyranometer, Model PSP - 14875 PF, from the Department of Mechanical Engineering, University of Nigeria, Nsukka. Readings of the latter were also taken at intervals of five minutes.

The Eppley pyranometer readings gave the cummulative insolation for the five-minute interval. By finding the difference between the readings for two consecutive intervals, the average instantaneous insolation for the intervals was obtained. Graphs of the average instantaneous insolation against the local time were plotted. These graphs are shown in figures 3.1.1 and 3.2.1 respectively for the two days while the instrument readings for these days are shown in tables 3.1 and 3.2 respectively.

The correlation between the graphs of the two instruments indicates that the constructed pyranometer is sufficiently sensitive.

TABLE 3.1 - INSTRUMENT READING FOR 19 - 4 - 91

LOCAL TIME	EPPLEY CUMMULATIVE INSOLATION (W H M^{-2})	EPPLEY CUMMULATIVE INSOLATION AT 5 MINUTES INTERVALS (W H M^{-2})	EPPLEY MEAN INSTANTANEOUS INSOLATION (W M^{-2})	INSTANTANEOUS PYRANOMETER READING (V) (GALVANOMETER DEFLECTION)
11.50	0	-	-	-
11.55	77	77	15.4	7.85
12.00	124	47	9.4	4.50
12.05	192	68	13.6	7.52
12.10	279	87	17.4	7.96
12.15	372	93	18.6	8.40
12.20	412	40	8.0	2.50
12.25	427	15	3.0	0.55
12.30	443	16	3.2	0.95
12.35	452	9	1.8	0.21
12.40	456	4	0.8	0.07
12.45	460	4	0.8	0.04
12.50	464	4	0.8	0.29
12.55	469	5	1.0	0.67
13.00	480	11	2.2	1.56
13.05	505/RESET	25	5.0	3.51
13.10	38	38	7.6	2.80
13.15	69	31	6.2	5.20
13.20	143	74	14.8	6.50
13.25	210	67	13.4	7.80
13.30	273	63	12.6	4.80
13.35	334	61	12.2	7.70
13.40	411	77	15.4	5.10
13.45	422	11	2.2	5.00
13.50	426	4	0.8	0.04
13.55	-	-	-	-
14.00	10	10	2.0	-

TABLE 3.1 (CONTINUED)

LOCAL TIME	EPPLEY CUMMULATIVE INSOLATION ($W H M^{-2}$)	EPPLEY CUMMULATIVE INSOLATION AT 5 MINUTES INTERVAL ($W H M^{-2}$)	EPPLEY MEAN INSTANTANEOUS INSOLATION ($W M^{-2}$)	INSTANTANEOUS PYRANOMETER READING (V) (GALVANOMETER DEFLECTION)
14.05	50	40	8.0	4.85
14.10	84	34	6.8	2.75
14.15	134	50	10.0	5.68
14.20	204	70	14.0	6.65
14.25	279	75	15.00	7.25
14.30	345	66	13.2	4.12
14.35	352	7	1.4	6.0
14.40	357	5	1.0	-
14.45	365	8	1.6	0.45
14.50	385	20	4.0	3.15
14.55	437	52	10.4	4.70
15.00	492	55	11.0	5.35
15.05	557	65	13.0	5.90

TABLE 3.2 INSTRUMENT READINGS FOR 20 - 4 - 91

LOCAL TIME	EPPLEY COMMULATIVE INSOLATION (W H M^{-2})	EPPLEY CUMMULATIVE INSOLATION FOR 5 MINUTES INTER-VAL (W H M^{-2})	EPPLEY MEAN INS-TANTANEOUS INSOLATION (W M^{-2})	INSTANTANEOUS PYRANOMETER READING (V) (GALVANOMETER OUTPUT)
11.20	21 75	-	-	0.237
11.25	22 08	33	6.6	0.217
11.30	22 44	36	7.2	0.215
11.35	22 70	26	5.2	0.210
11.40	22 87	17	3.4	0.206
11.45	23 09	22	4.4	0.210
11.50	23 44	35	7.0	0.221
11 55	23 75	31	6.2	0.218
12.00	23 99	24	4.8	0.215
12.05	24 25	26	5.2	0.213
12.10	24 49	24	4.8	0.217
12.15	24 81	32	6.4	0.218
12.20	25.12	31	6.2	0.217
12.25	25 39	27	5.4	0.218
12.30	25 68	29	5.8	0.217
12.35	25 93	25	5.0	0.215
12.40	26 17	24	4.8	0.215
12.45	26 44	27	5.4	0.216
12.50	26 78	34	6.8	0.222
12.55	27 22	44	8.8	0.228
13.00	27 78	56	11.2	0.237
13.05	28.27	49	9.8	0.227
13.10	28 55	28	5.6	0.210
13.15	28 76	21	4.2	0.209
13.20	29 01	25	5.0	0.212
13.25	29 31	30	6.0	0.216
13.30	29 60	29	5.8	0.217

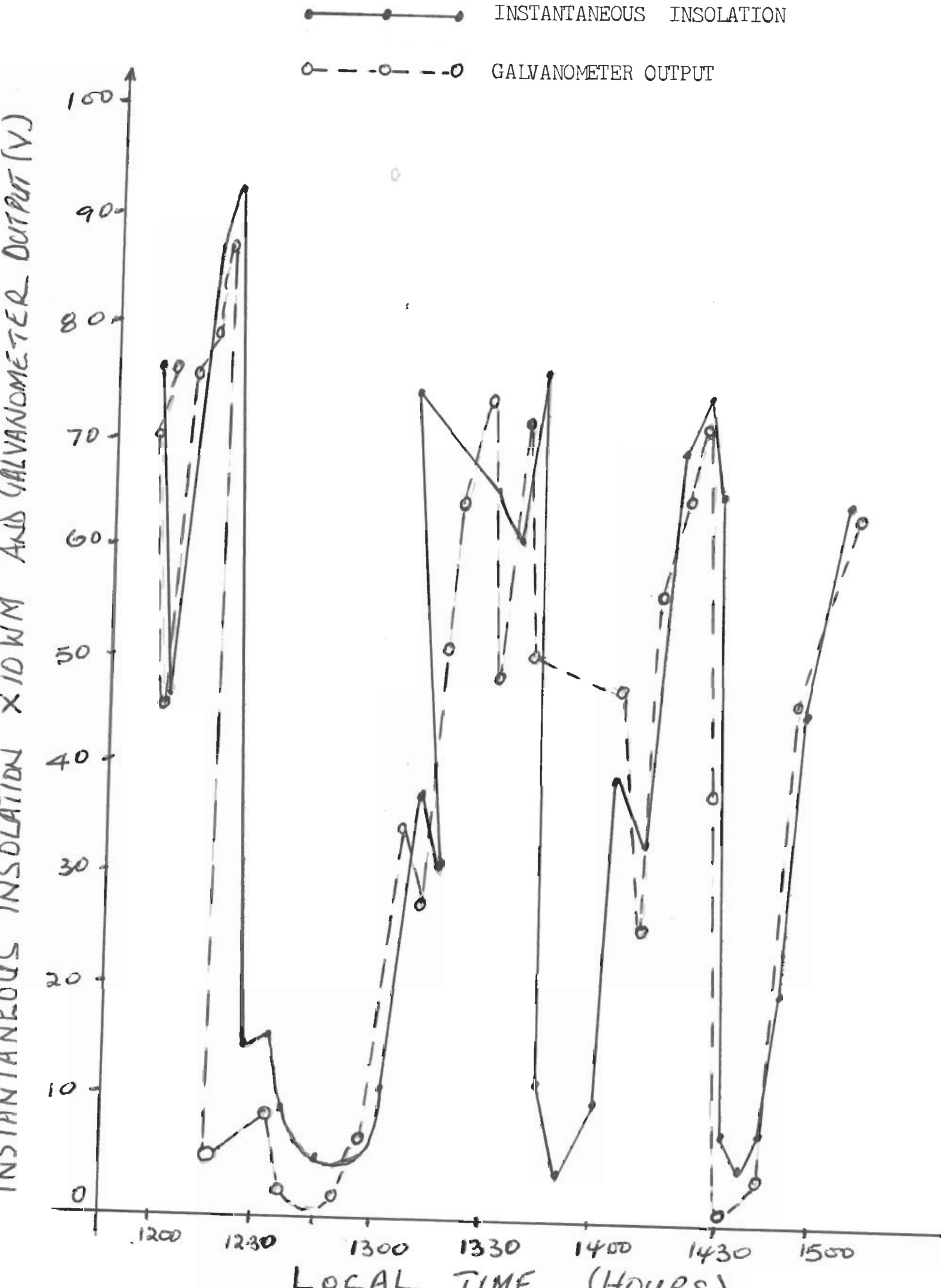
INSTANTANEOUS INSOLATION
GALVANOMETER OUTPUT
INSTANTANEOUS INSOLATION X10WM AND GALVANOMETER OUTPUT (V.)
100
90
80
70
60
50
40
30
20
10
0
1200
1230
1300
1330
1400
1430
1500
LOCAL TIME (HOURS)

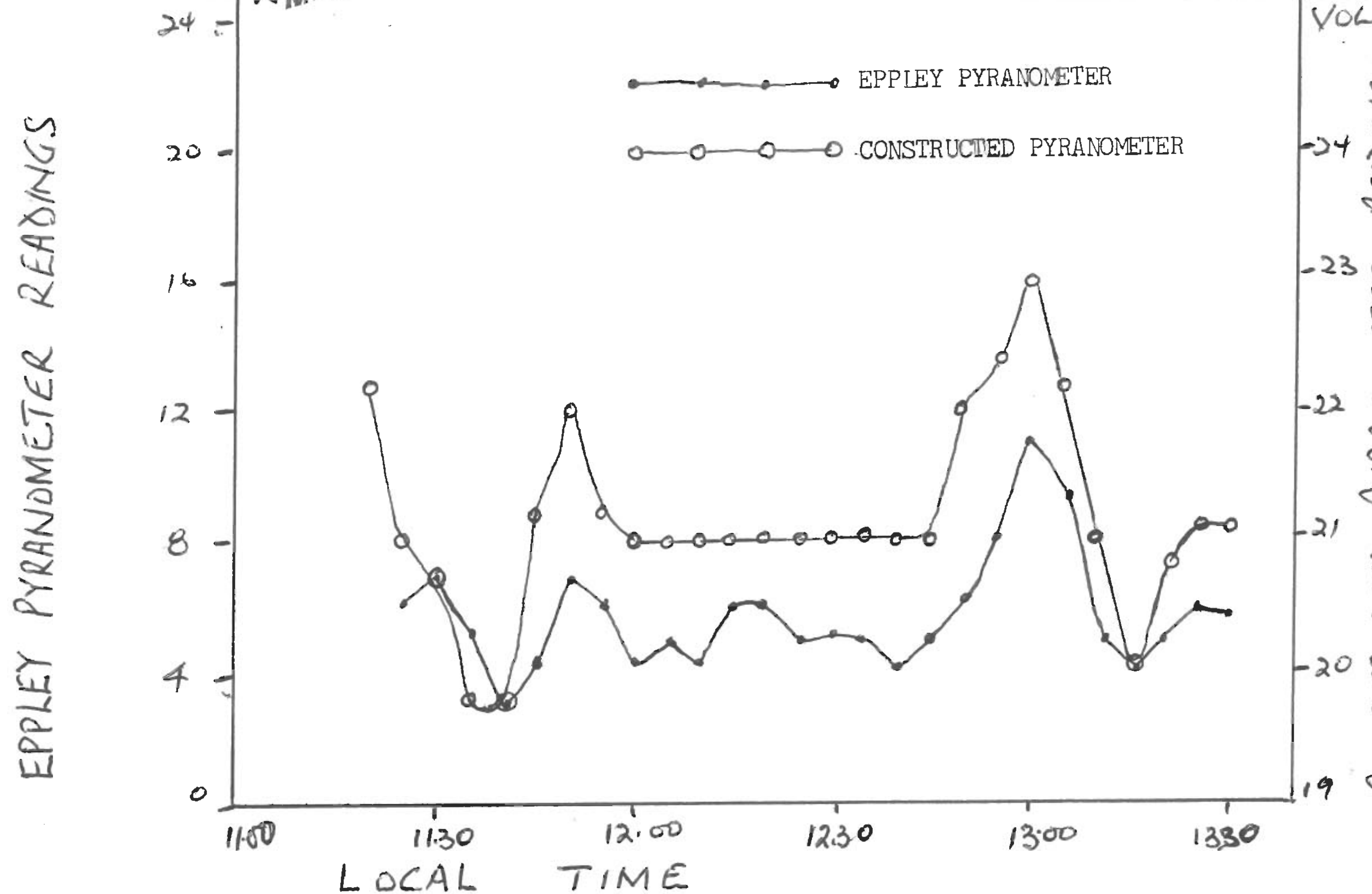

Fig. 3.2.1 VARIATION OF INTENSITY OF SOLAR RADIATION AND GALVANOMETER OUTPUT WITH LOCAL TIME

TABLE 3.3 GALVANOMETER DEFLECTION AT DIFFERENT LEVELS OF INSOLATION FOR THE CONSTRUCTED PYRANOMETER

MEAN INSTANTANEOUS. INSOLATION ($W M^{-2}$)	MEAN GALVANOMETER DEFLECTION (V) X 10
30	4.0
90	7.0
180	11.5
210	13.8
240	16.5
270	20.5
300	24.4
330	24.5
360	26.8
384	29.0
390	29.5
420	31.8
450	33.0
480	36.0
570	43.8
600	47.0
630	52.0
660	54.5
690	59.5
900	70.5
960	82.0
990	85.0
1050	85.0
1140	95.0

3.3 CALIBRATION CONSTANT

The constructed pyranometer is calibrated against a standard Eppley pyranometer. The calibrated readings are shown in Table 3.3.

These readings are plotted in fig. 3.3 .1 to obtain the calibration curves. The calibration curve for the constructed pyranometer has a slope 0.87 mm/W $M^{-2} \pm$ 1.2%. This means that when the intensity of solar radiation changes by 1 W M^{-2}, the galvanometer deflection changes by 0.87. The scale of the galvanometer is linear and graduated in mm and therefore a change of 0.87 mm can be detected. Thus our pyranometer responds well to changes in intensity of solar radiation.

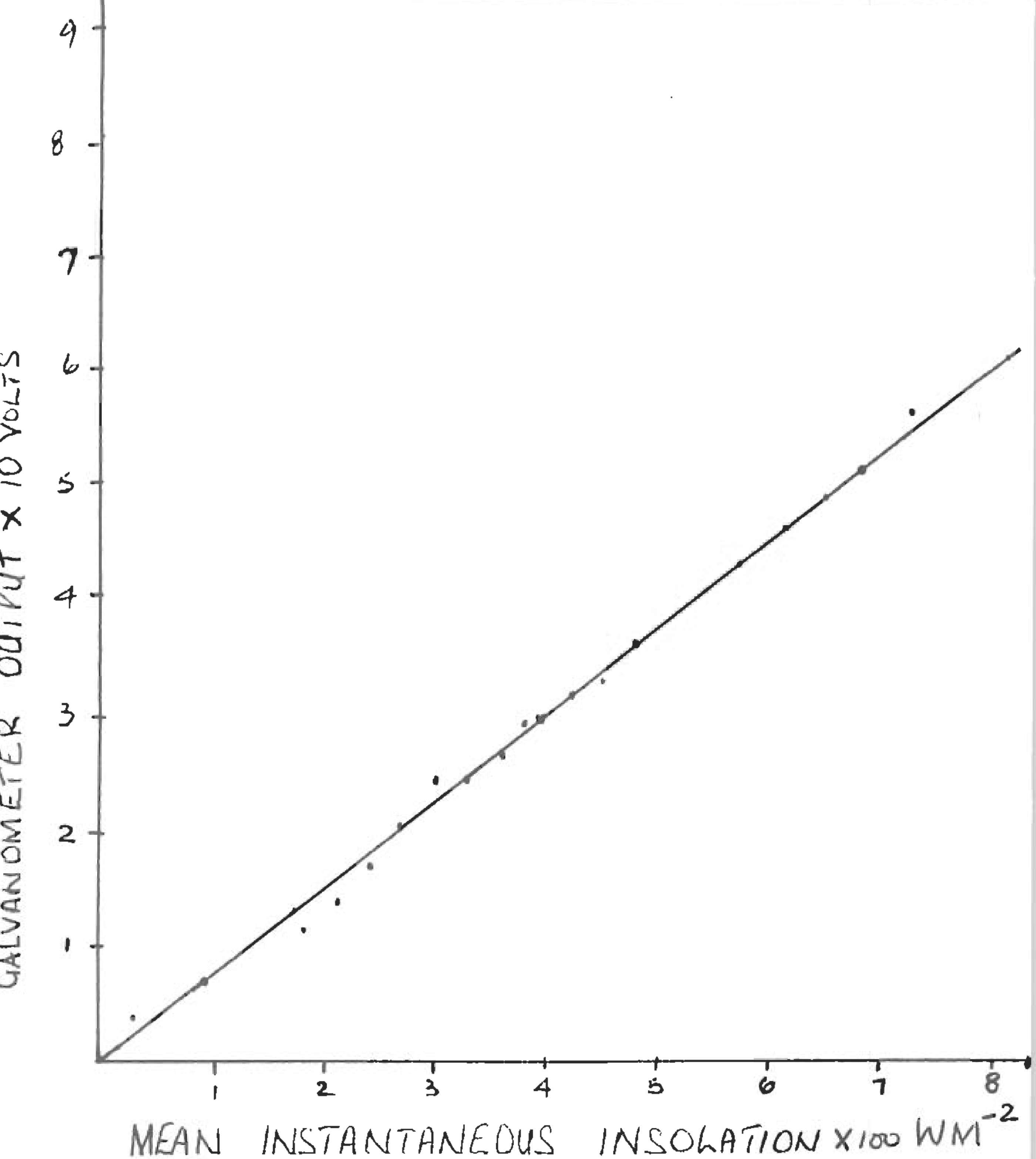

Fig. 3.3.1 CALIBRATION GRAPH FOR THE CONSTRUCTED PYRANOMETER

CHAPTER FOUR

4 . 0 MEASUREMENTS, ANALYSIS AND DISCUSSION

4 . 1 SOLAR RADIATION DATA FOR NSUKKA AS MEASURED WITH OUR PYRANOMETER

The instantaneous insolation at different hours of the day in Nsukka was measured for the month of May, 1991 using our pyranometer. The pyranometer deflection was recorded at each hour (local time). The corresponding instantaneous insolation is interpolated from the calibration graph.

TABLE 4.1 GLOBAL INSOLATION (WM^{-2}) DATA FOR NSUKKA FOR THE MONTH OF MAY, 1991

DATE	LOCAL TIME	GALVANOMETER OUTPUT (V)	INSTANTANEOUS INSOLATION (WM^{-2})
1-5-91	8 . 00	-	-
	9 . 00	-	-
	10 . 00	13 . 5	175
	11 . 00	12 . 5	165
	12 . 00	5 . 0	75
	13 . 00	9 . 5	130
	14 . 00	17 . 0	216
	14 . 30	10 . 5	140
	15 . 00	11 . 0	147
	16 . 00	11 . 5	153
	16 . 30	9 . 0	124
	17 . 00	13 . 2	172
2-5-91	8 . 00	-	-
	9 . 00	-	-
	10 . 00	58 . 5	700
	11 . 00	67 . 5	802
	11 . 30	65 . 5	780
	12 . 00	64 . 0	763
	12 . 30	63 . 5	756
	13 . 00	69 . 0	820
	14 . 00	17 . 0	216
	15 . 00	58 . 0	694
	16 . 00	13 . 4	174
	17 . 00	14 . 0	182

TABLE 4.1 (CONTINUED)

DATE	LOCAL TIME	GALVANOMETER OUTPUT (V)	INSTANTANEOUS INSOLATION (WM^{-2})
3-5-91	8 . 00	27 . 5	340
	9 . 00	41 . 5	501
	10 . 00	6 . 8	99
	11 . 00	6 . 5	81
	12 . 00	11 . 5	153
	13 . 00	10 . 0	135
	13 . 30	12 . 0	159
	14 . 00	68 . 0	810
	15 . 00	48 . 0	579
	15 . 30	32 . 0	392
	16 . 00	7 . 00	100
	16 . 30	8 . 00	111
	17 . 00	5 . 00	75
6-5-91	8 . 00	0 . 5	25
	8 . 30	1. 7	37
	9 . 00	7 . 5	105
	9 . 30	5 . 9	86
	10 . 00	8 . 4	115
	11 . 00	14 . 0	182
	12 . 00	16 . 5	210
	13 . 00	23 . 8	297
	13 . 30	17 . 2	219
	14 . 00	24 . 0	299
	14 . 30	22 . 6	280
	15 . 00	19 . 00	240
	16 . 00	13 . 0	170

TABLE 4 . 1 (CONTINUED)

DATE	LOCAL TIME	GALVANOMETER OUTPUT (V)	INSTANTANEOUS INSOLATION (WM^{-2})
9-5-91	8 . 00	1 . 9	39
	8 . 30	1 . 9	39
	9 . 00	2 . 7	50
	10 . 00	11 . 0	147
	11 . 00	11 . 0	147
	12 . 00	14 . 5	190
	13 . 00	21 . 0	264
	13 . 30	20 . 0	252
	14 . 00	29 . 0	357
	15 . 00	27 . 0	335
	16 . 00	16 . 0	205
	16 . 30	18 . 6	235
	17 . 00	2 . 3	43
10-5-91	8 . 00	8 . 2	111
	9 . 00	17 . 0	216
	10 . 00	19 . 0	240
	11 . 00	40 . 0	485
	12 . 00	38 . 0	462
	13 . 00	16 . 0	205
	13 . 30	20 . 0	252
	14 . 00	45 . 0	543
	14 . 30	18 . 0	228
	15 . 00	21 . 0	264
	15 . 30	20 . 0	257
	16 . 00	4 . 2	65
	17 . 00	3 . 6	60

TABLE 4. 1 (CONTINUED)

DATE	LOCAL TIME	GALVANOMETER OUTPUT (V)	INSTANTANEOUS INSOLATION (WM^{-2})
7-5-91	8 . 00	3 . 8	60
	9 . 00	8 . 9	121
	10 . 00	14 . 0	182
	11 . 00	23 . 0	287
	12 . 00	22 . 0	275
	13 . 00	12 . 0	159
	13 . 30	25 . 0	370
	14 . 00	-	-
	15 . 00	16 . 0	205
	16 . 00	-	-
8-5-91	8 . 00	0 . 8	28
	8 . 30	1 . 5	35
	9 . 00	3 . 3	52
	10 . 00	11 . 2	149
	11 . 00	19 . 0	240
	12 . 00	25 . 0	310
	13 . 00	46 . 5	560
	13 . 30	40 . 0	485
	14 . 00	18 . 0	228
	14 . 30	50 . 0	600
	15 . 00	32 . 0	392
	16 . 00	9 . 0	124
	17 . 00	2 . 3	43

TABLE 4 . 1 (CONTINUED)

DATE	LOCAL TIME	GALVANOMETER OUTPUT (V)	INSTANTANEOUS INSOLATION (WM^{-2})
13-5-91	8 . 00	8 . 7	120
	9 . 00	23 . 0	287
	10 . 00	6 . 1	88
	10 . 30	21 . 0	264
	11 . 00	8 . 2	112
	12 . 00	8 . 4	115
	12 . 30	24 . 8	308
	13 . 00	58 . 5	700
	13 . 30	57 . 0	580
	14 . 00	39 . 0	473
	15 . 00	-	-
	16 . 00	6 . 0	87
	16 . 30	4 . 1	65
	17 . 00	1 . 5	35
	17 . 30	-	-
14-5-91	8 . 00	-	-
	9 . 00	5 . 5	82
	9 . 30	9 . 5	130
	10 . 00	12 . 0	159
	10 . 30	25 . 0	310
	11 . 00	13 . 0	170
	11 . 30	33 . 0	403
	12 . 00	33 . 5	413
	13 . 00	25 . 0	310
	13 . 30	30 . 0	369
	14 . 00	21 . 0	264
	14 . 30	15 . 5	200
	15 . 00	31 . 5	385
	15 . 30	18 . 5	235
	16 . 00	11 . 5	152

TABLE 4 . 1 (CONTINUED)

DATE	LOCAL TIME	GALVANOMETER OUTPUT (V)	INSTANTANEOUS INSOLATION (WM^{-2})
16-5-91	8 . 00	15 . 0	194
	9 . 00	22 . 3	280
	9 . 30	15 . 0	194
	10 . 00	4 . 8	72
	10 . 30	22 . 0	275
	11 . 00	15 . 0	194
	11 . 30	18 . 0	228
	12 . 00	24 . 0	299
	12 . 30	53 . 5	640
	13 . 00	55 . 0	658
	14 . 00	1 . 8	39
	15 . 00	11 . 0	147
	16 . 00	7 . 9	110
	17 . 00	2. 7	50
20-5-91	8 . 00	16 . 0	205
	8 . 30	22 . 0	275
	9 . 00	28 . 0	345
	9 . 30	30 . 0	369
	10 . 00	33 . 0	403
	10 . 30	16 . 8	214
	11 . 00	36 . 0	440
	11 . 30	46 . 0	553
	12 . 00	10 . 0	135
	12 . 30	28 . 0	345
	13 . 00	19 . 0	240
	14 . 00	24 . 0	299
	15 . 00	30 . 0	369
	16 . 00	3 . 5	60
	16 . 30	6 . 4	95
	17 . 00	1. 2	30

TABLE 4. 1 (CONTINUED)

DATE	LOCAL TIME	GALVANOMETER OUTPUT (V)	INSTANTANEOUS INSOLATION (WM^{-2})
24-5-91	8 . 00	0 . 3	21
	8 . 30	0 . 4	22
	9 . 00	1 . 0	29
	10 . 00	45 . 0	543
	11 . 00	9 . 0	124
	12 . 00	10 . 0	135
	12 . 30	21 . 0	264
	13 . 00	29 . 0	355
	14 . 00	5 . 8	83
	15 . 00	13 . 0	170
	15 . 30	21 . 0	264
	16 . 00	14 . 0	182
	16 . 30	4 . 6	70
	17 . 00	3 . 3	52
	17 . 30	1 . 2	30
27-5-91	8 . 00	28 . 0	345
	8 . 30	24 . 0	299
	9 . 00	32 . 0	392
	9 . 30	33 . 0	403
	10 . 00	36 . 1	440
	10 . 30	41 . 0	495
	11 . 00	10 . 0	135
	12 . 00	18 . 0	288
	13 . 00	22 . 00	275
	13 . 30	11 . 0	147
	14 . 00	12 . 00	159
	14 . 30	14 . 0	182
	15 . 00	7 . 5	105

DATE	LOCAL TIME	GALVANOMETER OUTPUT (V)	INSTANTANEOUS INSOLATION (WM^{-2})
27-5-91. (Contd.)	16 . 00	7 . 1	100
	16 . 30	5 . 1	76
	17 . 00	3 . 5	58
	17 . 30	0 . 9	28
28-5-91	8 . 00	6 . 6	95
	8 . 30	4. 4	69
	9 . 00	8 . 9	120
	9 . 30	6 . 8	97
	10 . 00	22 . 0	275
	10 . 30	15 . 0	194
	11 . 00	27 . 0	334
	12 . 00	21 . 0	264
	13 . 00	25 . 0	310
	13 . 30	35 . 0	426
	14 . 00	32 . 0	392
	15 . 00	18 . 0	228
	16 . 00	1. 4	35
	17 . 00	0 . 1	20
29-5-91	8 . 00	-	-
	9 . 00	-	-
	13 . 00	19 . 0	240
	13 . 30	19 . 0	240
	14 . 00	16 . 0	205
	15 . 00	10 . 0	135
	15 . 30	6 . 9	99
	16 . 00	6 . 2	90
	16 . 30	7 . 2	101
	17 . 00	3 . 8	60

TABLE 4 . 1 (CONTINUED)

DATE	LOCAL TIME	GALVANOMETER OUTPUT (V)	INSTANTANEOUS INSOLATION (WM^{-2})
30-5-91	8 . 0	-	-
	9 . 00	10 . 0	135
	10 . 00	13 . 9	180
	11 . 00	34 . 0	416
	12 . 00	45 . 0	542
	13 . 00	5 . 0	75
	14 . 00	13 . 0	170
	14 . 30	30 . 0	252
	15 . 00	-	-
	15 . 30	14 . 0	182
	16 . 00	5 . 5	81
	16 . 30	7 . 8	109
	17 . 00	4 . 6	70
	17 . 30	1. 0	29
31-5-91	8 . 00	-	-
	8 . 30	3 . 0	52
	9 . 00	13 . 5	175
	10 . 00	14 . 0	182
	11 . 00	18 . 5	235
	12 . 00	20 . 0	252
	12 . 30	29 . 0	355
	13 . 00	18 . 0	228
	13 . 30	29 . 0	355
	14 . 00	15 . 0	194
	14 . 30	15 . 0	194
	15 . 00	13 . 0	170
	16 . 00	9 . 5	129
	16 . 30	8 . 8	120
	17 . 00	3 . 6	60

TABLE 4.2

MEAN HOURLY INSTANTANEOUS INSOLATION AT NSUKKA FOR THE MONTH OF MAY, 1991

(WM^{-2})

LOCAL TIME	07.00	07.30	08.00	08.30	09.00	09.30	10.00	10.30	11.00	11.30	12.00	12.30	13.00	13.30	14.00	14.30	15
MAY	-	-	131.9	103.5	192.5	213.2	244.1	292.0	267.6	491.0	283.4	444.8	331.2	316.2	291.0	259.5	28

4 . 2 DATA ANALYSIS AND DISCUSSION

The results of the measurements are tabulated in Tables 4.1 and 4.2. Table 4.2 shows the mean instantaneous insolation at different hours of the day for the period under investigation. An analysis of these data reveals the following:-

(i) Highest Instantaneous Intensity was 820 WM^{-2} recorded on the 2nd of May 1991 at 1300 hours local time.

(ii) Lowest Instantaneous Intensity was 20 WM^{-2} recorded on the 28th of May 1991 at 1700 hours local time.

(iii) Highest Mean Instantaneous Insolation was 491 WM^{-2} recorded at 1130 hours local time.

(iv) Lowest Mean Instantaneous Insolation was 29 WM^{-2} recorded at 1730 hours local time.

(v) In the absence of overcast clouds, the maximum intensity for a given day occurs between 1130 hours and 1300 hours local time.

4. 3 CONCLUSION

It has been successfully demonstrated that using locally available materials such as wood, copper plates, lampblack and glass, it is possible to construct an improved pyranometer that could be used to measure global radiation. The constructed pyranometer is estimated to cost ₦750 (seven hundred and fifty Naira). It is therefore cheap and simple as compared to imported ones. It is hoped that with better materials and improved technology, such as better copper plates for the sensor elements, better quality glass with high spectral transmission for the dome, highly skilled soldering of the thermocouples, a pyranometer almost as good as the standard Eppley pyranometer can be constructed.

4 . 4 SUGGESTIONS FOR FURTHER WORK

(i) ADAPTATION FOR MEASUREMENT OF COMMULATIVE INSOLATION

For the purpose of measuring cummulative insolation, it is suggested that the output of the pyranometer be connected to a sensitive automatic chart recorder.

The chart recorder plots the pyranometer output against time. An appropriate conversion factor can then be obtained by comparing the area under the graph with the cummulative insolation recorded by an Eppley pyranometer. The instantaneous insolation at a given time may also be obtained from the chart.

(ii) IMPROVEMENT OF RESPONSE TIME

The response time may be improved by:

a) using a material with low specific heat capacity (e.g platinum for making the sensor;

b) making the ratio of surface area to the thickness of the sensor as high as practicable;

c) the variation of the spectral composition of terrestrial global radiation has been well established by a number authors including GOLDBERG AN KLEIN[26], FRACECHINI and MAJOR[27]. It is suggested that such an investigation be carried out in our local environment so as to establish the pattern of this variation, on hourly and seasonal bases.

BIBLIOGRAPHY

1. MOLL, N.J.H. (1925), A Thermopile For Measuring Radiation, Proc. Phys. Soc. London Sect. B, 35.

2. DRUMMOND, A.J. and ROCHE, J.E. (1965) Corrections to be applied to Measurements made with Eppley (and others). Spectral Radiometers When Used With Schott coloured Glass, Filter. J. Apply Meteorol. 4, 741-744

3. MAC DONALD, J.H. (1951), SOME CHARACTERISTICS OF THE EPPLEY PYRHELIOMETER. Mon. Weather, Rev. 79, 153 - 159

4. H.L. PERMAN, ROTHAMSTED EXPL. station Report for 1973, pp. 172 - 201 (1974)

5. E. KLUGMAN and O.E. ONYEOGU,Energy Conversion and Management 19, 153, (1979)

6. C.E. Okeke and A.J. VARKEY, Measurement of Insolation Using Cds Photo resistor, Energy Conversion and Management, 21, pp. 267 - 273 (1981)

7. World METEOROLOGICAL ORGANISATION (1965). Guide to Meteorological Instruments and Observing Practices. W.M.O. No 8TP 3 GENEVA Switzerland.

8. W.J.H. MOLL, A Thermopile for Measuring Radiation Proc., Physics Soc. London. Seri. B 35, 257 - 260 (1923)

9. LANGLEY, S.P. (1900), The New Spectrum Ann. Rep. Smithson Inst. Pp. 683 - 692.

10. DORNO, C. (1922) Progress in Radiation Measurement, Mon. Weather. Rev. 50, 515 - 521.

11. GLAZE BROOK, SIR RICHARD "A Dictionary of Applied Physics" Vol. 3, pp. 699 - 719.

12. K. ANGSTROM, The absolute Determination of the Radiation of Heat With the Electric Compensation Pyrheliometer and Examples of the Application of this Instrument. Astrophysics J.d, 332 - 346 (1899).

13. C.G. ABBOT, The Silver Disc Pyrheliometer, Smithsonian Misc. Coll, 1911, 56 (19), 10.

14. H.H. KIMBALL and H.E. HOBBS. A new form of Thermo electric Recording Pyrheliometer; Mon. Weather Rev. 1923, 51. 239 - 242

15. M. WOLF. "Historical Development of Solar Cells" in solar cells, ed. C.E. Backus (New York: IEEE Press, 1976)

16. FABRIGTON DANIELS, DIRECT USE OF THE SUN's ENERGY, New Haven and London, Yalk University Press, P. 90 - 103.

17. MORGAN, C AND GRAIG, G.T.: "A Comparison of predicted Solar Insolation with Measured values at San Diego", SOLAR ENERGY, 18(b) 581 - 585 (1976)

18. LOF G.O.G., DUFFIE, J.A. AND SMITH, C.O., World Distribution of Solar Radiation, Engineering Experiment Station Report No. 21, University of Wincōnsin, Madison, Wonsonsin, July, 1966.

19. R. SIEGEL AND J.R. HOWELL, Thermal Radiation Heat transfer (New York: McGraw - Hill, 1972)

20. Encyclopaidic Dictionary of Physics 6, P. 521, Pergamon Press, New York, (1962)

21. M.P. THEKACKARA: The Solar Constant and the Solar Spectrum Measured from a Research Air craft, NASA Technical Report No. R. 351.

22. P.R. GAST, "Solar Radiation" in Hand book of Geophysics ed., C.F. Campenetal. (New York; Macmillam, 1960) PP. 14 - 16.

23. J.A. CHALDECOTH, Handbook Collection Relation to Head and Cold II, Catalogue of Exhibits With Description Note, Science Museum, H.M.S.O. London, (1954).

24. A.E. EZE, Construction and Use of a Sensitive Thermopile Pyranometer and Long Term Solar Radiation Parameters for some Urban Centres; An M.Sc. Thesis, University of Nigeria Nsukka, (1983).

19. R. SIEGEL AND J.R. HOWELL, Thermal Radiation Heat transfer (New York: McGraw - Hill, 1972)

20. Encyclopaidic Dictionary of Physics 6, P. 521, Pergamon Press, New York, (1962)

21. M.P. THEKACKARA: The Solar Constant and the Solar Spectrum Measured from a Research Air craft, NASA Technical Report No. R. 351.

22. P.R. GAST, "Solar Radiation" in Hand book of Geophysics ed., C.F. Campenetal. (New York; Macmillam, 1960) PP. 14 - 16.

23. J.A. CHALDECOTH, Handbook Collection Relation to Head and Cold II, Catalogue of Exhibits With Description Note, Science Museum, H.M.S.O. London, (1954).

24. A.E. EZE, Construction and Use of a Sensitive Thermopile Pyranometer and Long Term Solar Radiation Parameters for some Urban Centres; An M.Sc. Thesis, University of Nigeria Nsukka, (1983).